Chemical Geology 260 (2009) 112–128

Contents lists available at ScienceDirect

Chemical Geology

journal homepage: www.elsevier.com/locate/chemgeo

Highly siderophile element and ^{187}Os isotope systematics of Hawaiian picrites: Implications for parental melt composition and source heterogeneity

Thomas J. Ireland [a,*], Richard J. Walker [a], Michael O. Garcia [b]

[a] Department of Geology, University of Maryland, College Park, MD 20742 USA
[b] Department of Geology and Geophysics, University of Hawaii, Honolulu, Hawaii USA

ARTICLE INFO

Article history:
Received 24 May 2008
Received in revised form 16 November 2008
Accepted 9 December 2008

Editor: B. Bourdon

Keywords:
Platinum-group elements
Highly siderophile elements
Fractionation
D values
Parental melt composition
Hawaii
Os isotopes

ABSTRACT

Absolute and relative abundances of the highly siderophile elements (HSE) are reported for 52 Hawaiian picrites (MgO >13 wt.%) and 7 related tholeiitic basalts (~7–12 wt.% MgO) from nine volcanic centers (Mauna Kea, Mauna Loa, Hualalai, Loihi, Koolau, Kilauea, Kohala, Lanai and Molokai). The parental melts for all the volcanic centers are estimated to contain ~16 wt.% MgO. Samples with higher MgO contents contain accumulated olivine. Samples with lower MgO contents have lost olivine.

Osmium, Ir and Ru abundances correlate positively with MgO. These elements are evidently sited in olivine and associated phases (i.e. chromite and PGE-rich trace phases) and behaved compatibly during crystal-liquid fractionation of picritic magmas. Platinum, Pd and Re show poor negative correlations with MgO. These elements behaved modestly incompatibly to modestly compatibly during crystal-liquid fractionation. Effects of crustal contamination and volatile losses on parental melt compositions were likely minor for most HSE, with the exception of Re for subaerially erupted lavas. The HSE abundances for the parental melts of each volcanic center are estimated by consideration of the intersections of HSE-MgO trends with 16 wt.% MgO. The abundances in the parental melts are generally similar for most volcanic centers: 0.5±0.2 ppb Os, 0.45±0.05 ppb Ir, 1.2±0.2 ppb Ru, 2.3±0.2 ppb Pt, and 0.35±0.05 ppb Re. Samples from Loihi contain higher abundances of Pt, Pd and Re which may be a result of slightly lower degrees of partial melting. Hualalai parental melts have double the Os concentration of the other centers, the only discernable HSE concentration heterogeneity among these widely distributed volcanic centers.

Two types of HSE patterns are observed among the various picrites. Type-2 patterns are characterized by greater fractionation between IPGE (Os, Ir, Ru) and PPGE (Pt, Pd), with higher Pt/Ir and Pd/Ir ratios than Type-1 patterns. Both pattern types are present in most of the volcanic centers and do not correlate with MgO content. The differences between the two patterns are attributed to the inter-relationship between partial melting and crystal-liquid fractionation processes, and likely reflect both differences in residual sulfides and the loss of chromite-associated IPGE alloys or Mss during magma ascent.

The ranges in $^{187}Os/^{188}Os$ ratios obtained for rocks from each of these volcanic centers are in good agreement with previously published data. Variations in $^{187}Os/^{188}Os$ isotope ratios between volcanic centers must reflect ancient source heterogeneities. The variations in Os isotopic compositions, however, do not correlate with absolute or relative abundances of the HSE in the picrites. Minor source heterogeneities have evidently been masked by partial melting and crystal-liquid fractionation processes. There is no evidence of derivation of any picritic lavas from sources with highly heterogeneous HSE, as has been implied by recent studies purporting to explain ^{186}Os isotopic heterogeneities.

Published by Elsevier B.V.

1. Introduction

The highly siderophile elements (HSE; Os, Ir, Ru, Pt, Pd, Rh, Re and Au) have a high affinity for metallic Fe and, to a lesser degree, a high affinity for sulfides (Barnes et al., 1985; Walker, 2000). Abundances of HSE, coupled with Os isotopes ($^{187}Re \rightarrow {}^{187}Os + {}^{-}\beta$; $\lambda = 1.67 \times 10^{-11}\ yr^{-1}$), are important tools for characterizing the geochemical history of mantle reservoirs (Barnes et al., 1985; Brügmann et al., 1987; Barnes and Picard, 1993; Rehkamper et al., 1997, 1999; Brandon and Walker, 2005). The absolute and relative abundances of HSE in mantle rocks can be modified by, and therefore potentially be used to detect, diverse mantle processes including partial melting, melt refertilization, other forms of metasomatism, and crustal recycling (e.g., Rehkamper et al., 1997; Lassiter and Hauri, 1998; Rehkamper et al., 1999; Momme et al., 2003; Bockrath et al., 2004). Further, the core contains about 98% of the Earth's inventory of HSE with some models suggesting that the outer

* Corresponding author. Tel.: +1 301 422 6469; fax: +1 301 405 3597.
E-mail address: tireland@geol.umd.edu (T.J. Ireland).

0009-2541/$ – see front matter. Published by Elsevier B.V.
doi:10.1016/j.chemgeo.2008.12.009

core may contain ~300 times greater HSE abundances relative to the mantle (McDonough, 2003). Minor chemical exchange between the core and mantle could result in mantle with distinctive HSE and Os isotopic characteristics (Walker et al., 1995; Snow and Schmidt, 1998; Brandon and Walker, 2005).

Mantle plumes are typically defined as the focused, upward flow of mantle material originating at a boundary layer within the Earth (Morgan, 1971; Campbell and Griffiths, 1990). Generally, mantle plumes occur in intraplate settings (e.g. Hawaii, Deccan Traps), but are also present at mid-ocean ridges (e.g. Iceland). The sources of materials present in plumes, among other plume-related issues, remain highly controversial (Campbell and Griffiths, 1990; Anderson, 1998; Smith, 2003; Allègre and Moreira, 2004; Baker and Jensen, 2004; Schersten et al., 2004; Brandon and Walker, 2005). The abundances of the HSE in plumes could provide new insights to the origin and mechanics of plumes, given the numerous prior studies of plumes which have invoked the presence of materials as diverse as recycled crust and contributions from the outer core (Brandon et al., 1999; Lassiter and Hauri, 1998; Smith, 2003; Baker and Jensen, 2004, Schersten et al., 2004).

Here we consider HSE abundances and $^{187}Os/^{188}Os$ ratios in Hawaiian lavas. The Hawaiian mantle plume is an important example of intra-plate volcanism. It is the largest and hottest currently active plume (Sleep, 1990, 1992). Both geophysical and geochemical studies have suggested that the Hawaiian mantle plume may originate at the core–mantle boundary (Brandon et al., 1999; Montelli et al., 2004). Thus, the Hawaiian mantle plume has been the focus of numerous geochemical studies that have attempted to assess the chemical characteristics of the plume source (Eiler et al., 1996; Hauri et al., 1996; Lassiter and Hauri, 1998; Brandon et al., 1999; Norman and Garcia, 1999; Bennett et al., 2000; Humayun et al., 2004; Bryce et al., 2005; Sobolev et al., 2005; Nielsen et al., 2006; Bizimis et al., 2007). For example, some previous studies of $^{187}Os/^{188}Os$ ratios in Hawaiian basalts have concluded that recycled oceanic crust is an important component in the source region of the Hawaiian plume (Hauri et al., 1996; Lassiter and Hauri, 1998).

The absolute and relative HSE abundances in Hawaiian lavas have been considered in several studies. For example, Tatsumi et al. (1999) examined Mauna Loa and Kilauea tholeiites and hypothesized that the observed fractionation of the HSE resulted from the crystallization of phases such as chromite, olivine and clinopyroxene. They also suggested an important role for the separation of sulfides from the parental magmas. Bennett et al. (2000) studied the concentrations of several HSE along with $^{187}Os/^{188}Os$ ratios in a suite of picritic rocks from six Hawaiian shield volcanoes, several of which are included in the present study. They concluded that the variable HSE abundances in these picrites directly reflect plume source compositions, and suggested that residual sulfides in the plume source may be responsible for the absolute HSE abundance variations between the different Hawaiian volcanoes. They noted that the effects of the residual sulfides may obscure the contributions of various mantle HSE reservoirs to the plume.

To further efforts to better understand the HSE and ^{187}Os systematics of Hawaiian picrites, 52 picrites (MgO > 13 wt.%) were collected from nine volcanic centers (Mauna Kea, Mauna Loa, Hualalai, Loihi, Kilauea, Kohala, Koolau, Lanai and Molokai), including samples from both Hawaiian Scientific Drilling Project holes (HSDP-1 and -2). This sample suite represents some of the most primitive Hawaiian shield volcano melts. They may, thus, be particularly useful in preserving information about the concentrations of HSE in the mantle sources of the Hawaiian plume (Norman and Garcia, 1999). Seven related tholeiitic basalts (MgO ~ 7 to 12 wt.%), which are more evolved than the associated picrites, were also included in the study as a comparison for crystal-liquid fractionation processes. The objectives of this study are: (1) to better define the relative and absolute abundances of HSE in primitive plume-derived lavas, (2) to compare the concentrations of HSE in the parental melts for the different Hawaiian volcanic centers, (3) if differences are resolved, to identify the causes of HSE variations among these lavas, and (4) to identify whether there are resolvable differences in the HSE characteristics of the mantle sources, and if so evaluate their causes.

2. Samples

The samples analyzed in this study are predominantly primitive tholeiitic picrites, which are representative of the shield building stage of Hawaiian volcanism (Norman and Garcia, 1999). The picritic lavas were derived from high density melts that erupted on the flanks of the Hawaiian volcanoes, and may have bypassed the summit reservoirs of the volcanoes (e.g., Garcia et al., 1995). These rocks are, therefore, less likely to have been affected by fractionation processes that may operate in high level magma chambers. The degree of partial melting to produce the picrites has been estimated to range from 4 to 10% (Norman and Garcia, 1999).

Samples were obtained from submersible dives and submarine dredge hauls from the submerged flanks of the Hawaiian volcanoes, subaerial flows and from both Hawaiian Scientific Drilling Project holes (Table 1). Our samples are from nine Hawaiian volcanoes that span approximately 3 Myr of eruption history. All five of the Big Island volcanoes are represented (Kohala, Hualalai, Mauna Kea, Mauna Loa and Kilauea), along with samples from Loihi, Koolau (Oahu), Lanai and East Molokai. These samples were selected to provide a representative sampling of the HSE systematics for the Hawaiian picrites on both an intra- and inter-volcanic scale. Samples were collected as 100–400 g hand-sized masses, with the exception of the HSDP core samples (~100 to 200 g of rock chips and powders). For several HSDP samples, considerably smaller amounts of material were available (2–10 g for samples SR0683-5.75, SR0714-11.55, SR0750-12.45, SR0756-13.25, SR00762-4.60 and SR0846-2.80). These samples were only analyzed for abundances of Os and Re, as well as $^{187}Os/^{188}Os$ ratios. The majority of samples contain abundant phenocrysts of olivine (0.5 to 1.0 mm) in a fine grained matrix. Three more evolved samples (Lo 186-11, K98-08 and LWAW-7) also contain small amounts of plagioclase and clinopyroxene phenocrysts. Samples KOH-1-28, H-5, ML-2-50, Kil 1840, LO-02-02, LO-02-04, MK 1-6, H-11, H-23 and ML1868 were also studied by Bennett et al. (1996, 2000).

3. Analytical procedures

Visibly weathered surfaces on large hand samples were removed using a diamond rock saw. The samples were polished using SiC sandpaper to remove saw marks and were then broken into cm-sized chips using a high-tensile strength alloy mortar and pestle or with a ceramic-faced jaw crusher. These chips were screened again for weathered pieces and metal contamination. Finally, the samples were ground into a fine powder and homogenized using an agate shatterbox.

Major and trace element data for unpublished samples were obtained from the X-ray Laboratory at Franklin and Marshall College, which utilizes a Phillips 2404 XRF vacuum spectrometer. The accuracy and reproducibility of the analyses are estimated to be ~1% and ~5% for major and minor elements, respectively (Boyd and Mertzman, 1987).

Olivine compositions in polished thin sections were obtained using a JEOL JXA-8900 electron microprobe at the University of Maryland, using a 15 keV accelerating voltage, 20 nA beam current and a 10 μm spot size. A San Carlos olivine standard was analyzed concurrently with samples to monitor the external precision ($n = 30$). External precision (2σ) for SiO_2, FeO, MgO, CaO, NiO and MnO are 0.3%, 0.7%, 0.2%, 4.7%, 3.0% and 7.0% respectively. External precision (2σ) for other trace elements in olivine was 30% for Cr_2O_3, 13% for Al_2O_3 and 19% for CoO.

Methods used in this study for the separation of the HSE are based upon procedures outlined by Shirey and Walker (1995) and Cohen and Waters (1996). Samples were dissolved and equilibrated with spike

Table 1
Major element data for Hawaiian picrites

Volcano	Sample name	SiO_2 (wt.%)	TiO_2	Al_2O_3	FeO[d]	Fe_2O_3[d]	MnO	MgO	CaO	Na_2O	K_2O	P_2O_5	LOI	SUM	$Mg\#_{wr}$	Ref
Mauna Kea																
	MK-1-6[c]	49.21	2.04	9.83	11.46		0.18	17.24	7.29	1.76	0.39	0.22		99.62	74.9	1
HSDP-1	R189-8.5B	43.89	1.16	5.99		13.17	0.17	28.25	5.86	0.08	1.15	0.12		99.84	82.5	2
	R197-0.8B	45.63	1.54	7.27		13.19	0.18	23.77	6.66	0.26	1.47	0.16		100.13	79.9	2
	R215-7.2B	45.39	1.49	7.40		12.86	0.17	23.99	6.86	0.19	1.33	0.15		99.83	80.4	2
HSDP-2	SR0129-5.20[a]	46.57	2.88	15.64		13.17	0.18	6.93	11.76	2.19	0.25	0.28	0.26	99.85	53.7	3
	SR0328-3.10	44.66	1.25	6.22		12.81	0.17	27.19	5.81	1.09	0.20	0.13	−0.35	99.53	82.4	3
	SR0346–5.60	46.97	1.86	9.80		12.83	0.18	17.97	8.27	1.60	0.23	0.18	0.00	99.89	75.5	3
	SR0401-2.85	45.03	1.21	6.46		12.96	0.18	26.70	5.75	1.09	0.19	0.12	−0.21	99.69	81.9	3
	R0450-3.55	45.41	1.33	6.99		12.74	0.18	25.08	6.83	0.98	0.08	0.14	1.06	99.76	81.3	3
	SR0502-4.85	45.26	1.15	6.47		12.75	0.18	26.46	6.30	0.80	0.05	0.11	1.85	99.53	82.0	3
	SR0683-5.75	47.22	1.63	9.10		12.4	0.17	19.55	7.85	1.36	0.15	0.16	0.57	99.59	77.6	3
	SR0714-11.55[a]	49.69	2.33	12.73		12.26	0.18	9.36	10.80	2.00	0.26	0.23	0.18	99.84	62.7	3
	SR0720-18.25	46.96	1.63	8.82		12.53	0.17	20.40	7.42	1.47	0.21	0.17	−0.08	99.78	78.2	3
	SR0741-7.90	46.45	2.00	10.66		12.97	0.18	16.21	9.03	1.75	0.22	0.19	0.17	99.66	73.3	3
	SR0750-12.45	46.63	1.89	10.31		12.77	0.18	17.23	8.71	1.69	0.18	0.18	0.75	99.77	74.8	3
	SR0756-13.25	46.38	1.77	9.70		12.69	0.17	18.91	8.16	1.54	0.21	0.17	0.77	99.70	76.6	3
	SR0762-4.60	46.69	1.82	9.98		12.68	0.18	17.93	8.40	1.63	0.25	0.17	−0.10	99.73	75.7	3
	SR0846-2.80[a]	49.73	2.55	12.33		12.26	0.18	10.00	10.21	2.01	0.31	0.26	0.47	99.84	64.2	3
	SR0891-15.10[c]	46.45	1.52	8.19		12.63	0.18	22.04	7.20	1.24	0.09	0.15	1.30	99.69	79.3	3
	SR0940-18.35[c]	46.99	2.22	11.61		13.18	0.18	13.59	9.71	1.79	0.28	0.20	2.16	99.75	69.4	3
	SR0954-8.00[c]	47.67	1.97	9.64		12.3	0.17	18.03	8.01	1.65	0.23	0.20	0.85	99.87	76.3	3
	SR0964-4.30[c]	44.70	1.08	5.91		12.34	0.17	29.07	5.23	0.80	0.08	0.11	1.47	99.49	83.8	3
Mauna Loa																
	ML-2-50[c]	48.44	1.40	9.46	11.26		0.17	19.92	7.38	1.54	0.22	0.12		99.91	77.8	1
	ML KAH-1	47.81	1.53	8.83	11.47		0.18	21.66	6.68	1.47	0.25	0.15		100.03	78.9	1
	ML 1868-9	47.96	1.37	8.88	11.37		0.18	21.48	6.82	1.46	0.26	0.14		99.92	78.9	1
HSDP-1	R128-0.45	45.33	1.06	7.55		12.29	0.17	26.12	5.70	0.10	1.29	0.10		99.71	82.4	2
HSDP-2	SR0036-1.22	46.37	1.16	7.35		12.52	0.18	24.24	6.41	1.13	0.21	0.14	−0.32	99.71	81.0	3
	SR0040-1.07	45.54	1.00	6.31		12.58	0.17	27.28	5.54	0.97	0.20	0.12	−0.37	99.71	82.7	3
	SR0066-0.00	44.35	1.02	6.46		12.84	0.17	28.99	4.92	0.81	0.08	0.10	0.12	99.74	83.3	3
	SR0098-2.00	47.22	1.46	9.02		12.33	0.17	20.77	7.20	1.31	0.23	0.14	−0.38	99.85	78.8	3
	SR0117-4.00	46.70	1.69	9.85		13.05	0.18	19.42	7.41	1.44	0.08	0.18	0.24	100.00	76.6	3
Hualalai[c]																
	H-2	49.98	1.76	11.32	9.44	1.7	0.17	13.63	9.20	1.68	0.26	0.18	0.78	100.10	72.0	9
	H-5	49.70	1.67	11.09	11.12		0.18	14.93	8.71	1.71	0.26	0.15		99.52	72.7	1
	H-7[a]	50.21	1.86	12.18		11.93	0.17	11.23	9.76	1.92	0.30	0.17		99.73	67.5	4
	H-9[a]	50.18	1.87	12.15	9.47	1.52	0.17	11.30	9.84	1.85	0.29	0.18	0.84	99.66	68.0	9
	H-11	49.93	1.74	11.46	10.98		0.17	13.67	9.02	1.86	0.27	0.16		99.26	71.2	1
	H-23	46.01	1.08	7.37	11.57		0.17	25.80	5.69	1.19	0.19	0.10		99.17	81.5	1
	H-27	49.16	1.70	11.01	9.29	2.1	0.17	14.91	8.88	1.64	0.25	0.17	0.79	100.07	74.1	9
	H-P	46.76	1.33	8.10		12.56	0.17	23.19	6.09	1.17	0.19	0.14	−0.34	99.36	80.3	9
Loihi[c]																
	LO-02-02	44.63	1.40	7.13	11.95		0.19	24.21	6.33	1.34	0.40	0.14		97.72	80.1	1
	LO-02-04	44.14	1.31	6.40	10.22	1.58	0.17	26.58	5.70	1.03	0.33	0.15	2.27	99.88	82.3	9
	158-9	46.32	2.20	9.54		12.98	0.17	16.57	8.97	1.79	0.66	0.23	0.15	99.43	73.8	5
	186-5	44.24	1.75	8.43		12.85	0.17	19.52	10.50	1.55	0.47	0.18	−0.13	99.66	77.0	5
	186-11	43.21	2.66	12.05		13.45	0.17	13.76	9.58	3.16	1.21	0.44	0.54	99.69	69.3	5
	187-1	42.93	1.33	7.08		13.31	0.18	25.16	7.58	1.28	0.38	0.14	−0.24	99.37	80.6	5
Kilauea																
	KIL-1-18[c]	49.35	2.03	11.22	11.33		0.18	13.80	9.14	1.64	0.39	0.17		99.25	70.7	1
	KIL-2-3[c]	46.23	1.62	8.30	9.38	2.03	0.16	22.36	6.83	1.23	0.27	0.16	0.73	99.30	81.0	9
	KIL-2-4[c]	46.32	1.61	8.29	9.52	1.81	0.16	22.55	6.79	1.21	0.27	0.17	0.77	99.47	80.9	9
	KIL-3-1[c]	47.62	1.97	9.42	9.92	1.73	0.17	19.24	7.24	1.44	0.35	0.22	0.62	99.94	77.6	9
	KIL 1840-2	49.32	2.11	11.38	11.22		0.18	14.27	9.19	1.79	0.37	0.19		100.02	71.6	1
Koolau																
	K98-08	46.77	1.78	10.25	10.12	1.63	0.18	17.78	8.36	1.54	0.23	0.17	1.24	100.05	75.8	9
	S497-6[c]	46.95	1.41	8.87	9.82	2.27	0.18	21.55	6.81	1.47	0.21	0.12	0.52	100.18	79.6	6
	S500-5B[c]	47.98	1.30	9.04	8.74	2.13	0.16	21.22	6.31	1.64	0.31	0.16	1.07	100.06	81.2	6
	S500-5B[b,c]	45.26	1.36	8.11		13.26	1.62	21.21	5.85	1.20	0.26	0.22	1.57	99.92	77.9	9
Kohala[c]																
	KO-1-10	49.05	1.92	11.60	9.91	1.38	0.17	13.54	9.37	1.68	0.33	0.21	0.84	100.00	70.9	9
	KO-1-20[a]	50.14	2.28	12.88	9.17	1.94	0.18	9.60	10.19	2.09	0.41	0.27	0.92	100.07	65.1	9
	KOH-1-28	48.64	1.41	9.30	10.97		0.16	20.52	7.21	1.30	0.26	0.12		99.89	78.7	1
Lanai																
	LWAW-4	48.17	1.67	11.58		12.53	0.17	14.48	8.04	1.17	0.04	0.12	1.88	99.85	71.8	7
	LWAW-7[a]	49.24	1.96	12.80		12.82	0.17	11.69	8.91	1.46	0.10	0.17	1.00	100.32	66.8	7
Molokai[c]																
	S501-2	43.97	1.12	5.74	8.84	2.53	0.15	28.96	3.87	0.83	0.29	0.11	3.04	99.45	85.4	9

[1] Norman and Garcia, 1999 [2] Rhodes, 1996 [3] Rhodes and Vollinger, 2004 [4] Gurriet, 1988 [5] Garcia et al., 1995 [6] Tanaka et al., 2002 [7] West et al., 1992 [8] Chen et al., 1991 [9] this study.

[a] tholeiitic basalt (MgO <13 wt.%).

[b] sample affected by Mn-crust alteration.

[c] submarine sam.

[d] total Fe reported as FeO or Fe_2O_3 unless values for both are present.

solutions by acid digestion in Pyrex Carius tubes. Approximately 2.5 g of the finely powdered sample, 3 g of Teflon-distilled concentrated HCl and 6 g of Teflon-distilled concentrated HNO_3 were used in the digestion. Spike solutions enriched in ^{190}Os, ^{185}Re and a mixed ^{191}Ir-^{99}Ru-^{194}Pt-^{105}Pd spike were used. The Carius tubes were sealed with an oxygen–propane torch, agitated and placed in an oven at 240 °C for at least 48 h to digest the sample.

Osmium was separated from the aqueous phase using a carbon tetrachloride (CCl_4) solvent extraction technique. Osmium was then back-extracted from the CCl_4 into concentrated HBr (Cohen and Waters, 1996), prior to a final microdistillation step to further purify the sample (Birck et al., 1997). The other HSE were separated from the aqueous phase by anion exchange chromatography using 2 mL of Eichrom AG1X8 anion exchange resin. After several cleaning steps, Re and Ru were collected in 10 mL of 6N HNO_3. Iridium and Pt were collected in 15 mL of concentrated HNO_3. The final cut, containing Pd, was collected in 15 mL of concentrated HCl.

Isotopic measurements of the HSE were completed using two types of mass spectrometers. Osmium concentrations and isotopic compositions were measured by negative thermal ionization mass spectrometry using either a single collector NBS-style mass spectrometer, or a VG Sector-54 mass spectrometer, both at the University of Maryland's Isotope Geochemistry Laboratory. Following microdistillation, sample Os was loaded onto a Pt filament along with $Ba(OH)_2$, and then heated to ~830 °C. External precision for $^{187}Os/^{188}Os$ ratios on repeat analyses of an Os standard solution was ±0.2% (2σ). Internal precision on individual samples was generally less than 0.2% ($2\sigma_m$). Osmium blanks averaged 3±1 pg and an $^{187}Os/^{188}Os$ of 0.18±0.06 (n=8). Because of the high Os concentrations of the samples, blank corrections for Os were minimal. Age corrections do not modify the $^{187}Os/^{188}Os$ obtained.

The other HSE were analyzed by inductively coupled plasma mass spectrometry (ICP-MS) using a Nu Plasma mass spectrometer, at the Plasma Mass Spectrometry Lab at the University of Maryland. Following purification of the HSE via anion exchange chromatography, each of the HSE was analyzed in a static mode using 2 or 3 electron multipliers. Sample and standard solutions were interspersed throughout the analytical sessions to monitor and correct for instrumental fractionation. Samples were diluted so that signals for the spike isotopes were between 1 and 5 mV. Well-characterized solutions of HSE separated from spiked iron meteorites that were diluted to give signals similar to the samples were occasionally measured to monitor accuracy. External precision (2σ) of these meteoritic standard solutions ranged between 1 and 5% for all elements (n=3). The total procedural blanks for the analyzed elements averaged: 5±3 pg Ir, 14±6 pg Ru, 540±230 pg Pt, 140±60 pg Pd and 4±2 pg Re (n=5). Platinum and Pd blanks improved throughout the analytical session, as an internal cleaning step of the Carius tubes was implemented. All analyses were blank corrected. Duplicates performed on separate aliquots of the same sample powder demonstrated reproducibility ranging from ±1 up to 20% for Re, Ir, and Ru, and up to 30% for Pt and Pd. The larger discrepancy between duplicate runs likely indicates small-scale heterogeneities in the distribution of the HSE within aliquots of sample powder, commonly termed the "nugget effect"; however, the chondrite-normalized HSE patterns are similar between poorly reproduced samples, indicating that this had only a minor effect on the conclusions reached.

Several samples in this study were previously analyzed for some of the HSE by Bennett et al. (1996, 2000). In general, most of the HSE were within 30% of the prior results, however, larger discrepancies as great as 100% were observed. The largest discrepancies were observed between Re abundances, and to a lesser extent, Pt and Pd abundances. The explanation for these discrepancies is not immediately clear, since both studies yielded reproducible results. There are at least three possible causes for the differences. First, different powders were analyzed in each study, prepared from different pieces of the same rock. Therefore, the differences may be a result of heterogeneities in the distribution of HSE carrier phases in these picritic rocks. This scenario is more likely to account for discrepancies in the platinum-group elements (PGE), rather than Re. Second, the largest inconsistencies for Re occur in subaerially-erupted samples. Rhenium can be lost as a volatile phase via igneous processes (Lassiter, 2003; Sun et al., 2003; Norman et al., 2004). Volatile loss is likely to be greater in subaerially-erupted samples. Third, Bennett et al. (2000) indicated that Carius tube digestion may result in incomplete dissolution of silicate phases, which may also retain a Re component. They implemented an added HF-digestion step to dissolve these phases, which resulted in variations of up to 100% with the Bennett et al. (1996) study. Despite differences in the absolute abundances of HSE, the chondrite normalized HSE patterns reported from the Bennett et al. (2000) study are generally similar to the HSE patterns observed in the present study. These minor differences do not impact our conclusions.

4. Results

Major element data for the 52 picrites and 7 tholeiitic basalts are presented in Table 1. Whole rock Mg#s ($\frac{Mg}{Mg^{2+}+Fe^{2+}}*100$) for the entire sample suite range from 53.7 to 85.4. The Mg#s have been shown to directly correlate with the abundance of olivine phenocrysts in analogous picritic samples (Norman and Garcia, 1999). Average olivine core compositions for each rock are reported in Table 2. Typical olivines tend to be normally zoned and have core forsterite (Fo) contents between Fo_{85} and Fo_{90}, with the Fo content typically remaining consistent for multiple grains in the same thin section. More evolved samples (SR0129-5.20, SR0714-11.55, SR0846-2.80 and LWAW-4) generally contain olivine with lower Fo contents (81 to 85).

The HSE and $^{187}Os/^{188}Os$ data are reported in Table 3. Absolute abundances of HSE in all of the picrites are generally greater than MORB, and in some cases approach the concentrations observed in peridotites and komatiites (Figs. 1 and 8). With the exception of Re, concentrations of HSE in all samples are less than estimates for primitive upper mantle (PUM; Becker et al., 2006; Fig. 1). The HSE concentrations in the Hawaiian picrites are generally consistent with abundances reported for other picrites worldwide (Bennett et al., 2000; Rehkamper et al., 1999; Momme et al., 2003).

Two general types of HSE patterns are observed in CI chondrite-normalized HSE diagrams (Fig. 1). Type-1 patterns are roughly similar to the shape of the PUM pattern, albeit with lower overall HSE abundances and higher relative and absolute abundances of Re. This pattern is characterized by lower Pt/Ir and Pd/Ir ratios than Type-2 samples, as well as a highly reproducible Os-Ir-Ru pattern. It is best observed in most Mauna Kea samples, but is also observed in picrites from all volcanic centers except Loihi and Lanai. Subaerially erupted samples have substantially lower Re abundances.

Type-2 HSE patterns are comparatively flat for Os, Ir, and Ru, but have higher absolute and relative abundances of Pt, Pd and Re. This type of pattern is best observed for Loihi samples, but is also observed in all volcanic centers (except Molokai) and all of the lower MgO tholeiitic basalts. It is characterized by more highly fractionated Pt/Ir and Pd/Ir ratios than Type-1 samples. This pattern shape is broadly similar to that for MORB and Pacific oceanic crust, although absolute Os, Ir, Ru, Pt and Pd abundances are much higher in the picrites (Tatsumi et al., 1999; Peuker-Ehrenbrink et al., 2003).

When considering data for the entire picrite suite, Os, Ir and Ru are positively correlated with MgO (Fig. 2). These correlations are clearly defined for picrites from most individual volcanic centers. Data for these elements generally plot within the range of compositions defined by samples from the Kilauea Iki lava lake, which originated as a differentiation sequence of ponded lava with an initial MgO content of ~15 wt.% (Wright, 1973; Pitcher et al., in press). Extensive differentiation processes at Kilauea Iki produced rocks with <5 to nearly 30 wt.% MgO (Helz, 1987). In our picrite suite, Pt, Pd and Re generally show slightly negative correlations with MgO (Fig. 2), but with significant scatter. Again, most data overlap with the range of concentrations present in

samples of Kilauea Iki. Notable inter-volcanic differences include higher Os abundances in Hualalai and higher Pt, Pd and Re abundances in Loihi samples.

Variations in $^{187}Os/^{188}Os$ ratios are modest within most volcanic centers (maximum variations of ~3.5%); however, there are significant differences between the volcanic centers (Fig. 3). Our results are consistent with those previously reported (Martin et al., 1994; Bennett et al., 1996; Hauri et al., 1996; Hauri and Kurz, 1997; Lassiter and Hauri, 1998; Brandon et al., 1999; Bennett et al., 2000; Bryce et al., 2005). Of note, Mauna Kea samples have the lowest $^{187}Os/^{188}Os$ ratios spanning a narrow range from 0.1287 to 0.1307. Mauna Loa, Hualalai, Loihi and Lanai all have significantly more radiogenic $^{187}Os/^{188}Os$ ratios with an upper limit (with one exception) of 0.1384 for sample LWAW-4 from Lanai. There are no correlations between $^{187}Os/^{188}Os$ ratios and MgO content within volcanic centers.

Sample S500-5B from the Koolau volcano, has a very strong enrichment in Pt (~8 ppb) relative to the other samples, as well as a significantly elevated $^{187}Os/^{188}Os$ (~0.26). This sample also has an elevated MnO content (1.62 wt.%), suggesting that Mn-crust material was present as a contaminant.

5. Discussion

Absolute and relative abundances of HSE in the Hawaiian picrite suite vary within and among each volcanic center (Table 3; Figs. 1 and 2). A major objective of this study is, therefore, to assess whether these variations are all process-related or reflect source heterogeneities. Processes such as crystal-liquid fractionation, during both partial melting and crystallization, and crustal contamination are major controls on HSE abundances in mafic through ultramafic systems

Table 2
Average olivine core chemistry for Hawaiian picrites

Volcano	Sample name	SiO_2 (wt.%)	Al_2O_3	FeO	MnO	MgO	CaO	NiO	Cr_2O_3	CoO	SUM	$Mg\#_{ol}$
Mauna Kea												
	MK-1-6[c]	40.36	0.05	12.33	0.19	46.63	0.21	0.37	0.09	0.03	100.26	87.1
HSDP-2[a]	SR0129-5.20[b]	39.29	0.05	17.72	0.24	42.53	0.31		0.03		100.21	81.1
	SR0450-3.55	40.44	0.05	13.57	0.19	45.82	0.23		0.08		100.43	85.7
	SR0502-4.85	36.95	0.07	12.97	0.19	48.45	0.23		0.12		98.99	86.9
	SR0683-5.75	40.51	0.08	11.90	0.16	46.86	0.25		0.09		99.86	87.5
	SR0714-11.55[b]	39.16	0.03	16.79	0.21	44.12	0.27	0.24	0.05		100.88	82.4
	SR0741-7.90	38.96	0.04	13.97	0.17	45.70	0.23	0.32			99.38	85.3
	SR0750-12.45	39.07	0.04	13.53	0.17	45.73	0.21	0.31			99.05	85.8
	SR0756-13.25	39.34	0.04	12.33	0.15	47.10	0.23	0.37			99.56	87.2
	SR0846-2.80[b]	39.44	0.79	15.48	0.20	43.88	0.27	0.30	0.06		100.43	83.5
	SR0891-15.10[c]	41.02	0.06	11.23	0.15	47.94	0.23	0.40	0.10		101.14	88.4
Mauna Loa												
	ML-2-50[c]	40.38	0.05	9.46	0.13	49.27	0.20	0.56	0.08	0.04	100.19	90.3
	ML KAH-1	40.51	0.05	9.54	0.14	49.34	0.20	0.49	0.10	0.03	100.40	90.2
	ML 1868-9	40.21	0.06	11.05	0.16	48.31	0.21	0.38	0.09	0.04	100.52	88.6
HSDP-2[a]	SR0040-1.07	39.34	0.03	14.18	0.18	45.48	0.28		0.07		99.59	85.1
	SR0117-4.00	39.52	0.03	15.27	0.24	44.57	0.26		0.06		99.96	83.9
Hualalai[c]												
	H-2	40.42	0.06	10.97	0.16	47.97	0.21	0.39	0.08	0.03	100.30	88.6
	H-5	40.40	0.06	11.04	0.16	48.05	0.20	0.42	0.09	0.02	100.43	88.6
	H-7[b]	40.41	0.05	11.33	0.16	47.76	0.22	0.37	0.09	0.03	100.42	88.3
	H-9[b]	40.30	0.06	10.73	0.16	47.88	0.20	0.39	0.10	0.03	99.85	88.8
	H-11	40.32	0.06	11.69	0.16	47.29	0.21	0.36	0.08	0.03	100.19	87.8
	H-23	40.53	0.05	11.30	0.18	47.46	0.21	0.38	0.08	0.03	100.22	88.2
	H-27	40.58	0.06	10.64	0.15	48.29	0.21	0.41	0.09	0.03	100.46	89.0
	H-P	40.52	0.06	12.01	0.16	47.17	0.20	0.40	0.07	0.03	100.61	87.5
Loihi[c]												
	LO-02-02	40.33	0.04	11.68	0.17	47.31	0.28	0.34	0.08	0.04	100.27	87.8
	LO-02-04	40.23	0.05	12.76	0.20	46.29	0.32	0.32	0.06	0.03	100.26	86.6
	158-9	40.41	0.04	10.29	0.15	48.53	0.25	0.41	0.08	0.04	100.19	89.4
	186-5	40.03	0.05	12.30	0.19	46.67	0.32	0.26	0.05	0.03	99.91	87.1
	186-11	39.55		14.00	0.21	45.59		0.27			99.62	85.3
	187-1	40.24	0.05	11.84	0.17	47.36	0.30	0.30	0.07	0.04	100.35	87.7
Kilauea												
	KIL-1-18[c]	40.14	0.06	10.36	0.14	48.35	0.22	0.45	0.09	0.04	99.85	89.3
	KIL-2-3[c]	40.18	0.05	10.51	0.15	48.11	0.23	0.44	0.08	0.03	99.78	89.1
	KIL-2-4[c]	40.79	0.06	9.84	0.12	48.89	0.23	0.45	0.09	0.03	100.51	89.9
	KIL-3-1[c]	40.25	0.07	11.61	0.15	47.60	0.22	0.42	0.09	0.04	100.45	88.0
	KIL 1840-2	40.17	0.06	11.55	0.15	47.80	0.22	0.44	0.09	0.04	100.50	88.1
Koolau												
	K 98-08	40.11	0.04	14.06	0.19	45.74	0.22	0.36	0.06	0.04	100.81	85.3
	S497-6[c]	40.70	0.05	11.26	0.17	47.78	0.19	0.41	0.09	0.02	100.67	88.3
	S500-5B[c]	40.55	0.05	11.29	0.16	47.98	0.18	0.36	0.08	0.03	100.69	88.3
Kohala[c]												
	KO-1-10	40.49	0.04	12.47	0.20	46.95	0.23	0.30	0.05	0.05	100.79	87.0
	KO-1-20[b]	40.68	0.06	11.47	0.18	47.26	0.22	0.38	0.07	0.03	100.36	88.0
	KOH-1-28	40.88	0.05	10.68	0.18	48.37	0.20	0.41	0.08	0.02	100.86	89.0
Lanai												
	LWAW-4	39.33	0.04	15.40	0.19	44.87	0.18	0.46	0.05	0.04	100.57	83.9
	LWAW-7[b]	40.21	0.06	11.25	0.15	47.92	0.20	0.48	0.07	0.04	100.37	88.4
Molokai[c]												
	S501-2	40.64	0.06	10.90	0.17	48.05	0.22	0.36	0.09	0.03	100.51	88.7

[a] HSDP olivine analyses from Putirka et al., 2007.
[b] tholeiitic basalt (MgO <13 wt.%).
[c] submarine sample.

(Barnes et al., 1985; Crocket and MacRae, 1986; Brügmann et al., 1987; Barnes and Picard, 1993; Rehkamper et al., 1997; Rehkamper et al., 1999; Crocket, 2000; Puchtel and Humayun, 2001; Maier et al., 2003; Momme et al., 2003; Bockrath et al., 2004; Maier and Barnes, 2004; Puchtel et al., 2004; Ballhaus et al., 2006). Volatile losses in subaerial and shallow submarine flows can also affect abundances of Re and perhaps Ir (Zoller et al., 1983; Sun et al., 2003; Lassiter, 2003; Norman et al., 2004). The effects of these processes must first be considered prior to a search for heterogeneities in the sources of these rocks.

5.1. Estimation of parental melt compositions

Estimation of a parental melt composition can be helpful in trying to deconvolve the effects of crystal-liquid fractionation on HSE abundances. The parental melt represents the most primitive magma that was produced directly from the melting of the mantle source region. Samples that have major element compositions that approach the estimated parental melt compositions are presumed to have experienced limited crystal-liquid fractionation following separation from their mantle sources (Norman and Garcia, 1999). Consequently, these samples may best preserve the HSE composition of the parental melt. Samples that deviate from the parental melt composition likely have experienced variable amounts of crystal-liquid fractionation or crustal contamination.

5.1.1. Parental melt composition and olivine fractionation

Norman and Garcia (1999) analyzed a subset of samples from the current study, including samples from Mauna Kea, Mauna Loa, Hualalai, Loihi, Kilauea and Kohala. They concluded that the parental melt compositions of the Hawaiian picrites for all volcanic centers in their sample suite likely contained at least 13–17 wt.% MgO. Considering that olivine is the only major liquidus phase in these rocks, samples with higher MgO (up to 29.1 wt.%) contents were presumed to have incorporated cumulate olivine, and samples with lower MgO contents were presumed to have lost olivine. A log–log variation diagram of Al_2O_3 (an incompatible element in olivine) versus MgO (a compatible element in olivine; Fig. 4) was used by Norman and Garcia (1999) to discriminate between samples related by olivine accumulation versus fractional crystallization. A break in slope for their entire sample suite was present at ~15 to 16 wt.% MgO and ~10 wt.% Al_2O_3, which roughly marks the estimated composition of the parental melt (Norman and Garcia, 1999). Our new data, for all volcanic centers, indicates a similar break in slope at ~16 wt.% MgO and ~11 wt.% Al_2O_3 which is generally consistent with this previous result. Although it would be advantageous to examine this relationship for samples from each volcanic center, there are either not enough samples, or insufficient spread in MgO contents within a suite, to make individual estimates of parental melt composition.

Parental melt compositions can also be inferred from the Fo contents of olivine phenocrysts. Assuming that $\frac{(Fe/Mg)_{ol}}{(Fe/Mg)_{wr}} = = 0.3$ (Roeder and Emslie, 1970; Putirka, 2005) and 10% Fe^{3+} (relative to total Fe) for the whole rock (Rhodes and Vollinger, 2004), the MgO content of a melt in equilibrium with olivine can be estimated. High Fo content olivine ($Fo_{86–90}$) would be in equilibrium with melts that contain approximately 13–16% MgO. Several of the picrites we studied have MgO contents within this range and probably approximate the parental melts of the picrites. Samples that fall within this range of MgO, and that are also in equilibrium with associated olivine core compositions, include samples H-2, H-5, H-9, H-11, H-27, Lo 158-9 and Kil 1-18 (Fig. 5).

Despite evidence that some whole rock samples may record primary magma compositions, it is also clear that variable proportions of olivine accumulation and removal have played an important role in the generation of these picrites. An estimate of the maximum amounts of olivine accumulation and removal for the remaining samples was deduced from the primary magma calculations above, assuming that parental melts contain 16 wt.% MgO (Table 4). For samples believed to have lost olivine via fractional crystallization, equilibrium olivine was mathematically added in 0.1% increments until the calculated olivine composition corresponded to the most magnesian olivine in the sample suite, following the procedure outlined by Danyushevsky et al. (2000). We chose Fo_{90} because this olivine composition corresponds to the most magnesian olivine present in the sample suite, and is in equilibrium with a whole rock MgO content of 16 wt.%. From this calculation, the maximum percentage of olivine removal is estimated to be ~37% (sample SR0129-5.20 from Mauna Kea, with a MgO content of 6.9 wt.%). For samples that have accumulated olivine, the amount of accumulation was estimated by mathematically subtracting Fo_{90} from the sample. This procedure was repeated until the sample composition calculated was in equilibrium with olivine of this composition (Fo_{90}). The maximum percentage of olivine accumulation is estimated to be 27% (sample SR0964-4.30 from Mauna Kea, with a MgO content of 29.1 wt.%).

Hereafter, the parental melts for all the Hawaiian shield volcanoes included in this study are assumed to contain 16 wt.% MgO. It is important to note, however, that this estimate is based on a data array for all the shield volcanoes analyzed in this study. There may be small differences in the MgO content of parental melts between individual volcanoes.

5.1.2. Volatile loss of Re

The volatile loss of Re during magma degassing in subaerially erupted lavas has previously been recognized in arc magmas (Sun et al., 2003) and in Hawaiian lavas (Lassiter, 2003; Norman et al., 2004). This same effect might be observed in the chondrite-normalized HSE patterns for Mauna Kea and, to a lesser extent, for Mauna Loa. In general, the chondrite-normalized HSE patterns for the picritic suite show sharp enrichments of Re. However, in the subaerially and shallow submarine erupted lavas from the HSDP drill core for Mauna Kea (R189-8.5B, R197-0.8B, R215-7.2B, SR0328-3.10 and SR0401-2.85), the chondrite-normalized HSE patterns show relative depletions of Re, consistent with loss from the flows. The picrites from the Mauna Loa portion of the HSDP samples do not show such dramatic depletions in Re abundances, but likely effects can be observed in samples SR0066-0.00 and SR0098-2.00. Lavas that were erupted in deep submarine settings (>2000 m below sea level) do not show obvious depletions in Re abundances and are presumed to have retained most or all of the Re from the melt (Table 1). Based on the depth of recovery of dredged samples, samples from Hualalai, Loihi, Kilauea (with the exception of subaerial erupted Kil 1840-2) and Koolau are presumed to have retained Re. Samples with significant Re volatile loss are not considered in the following section, where the Re abundances of the parental melts for each volcanic center are estimated.

Iridium abundances in Mauna Kea and Mauna Loa were also found to be somewhat variable with respect to MgO. Some of this variability may be due to minor volatile loss of Ir in subaerially erupted samples (Zoller et al., 1983). Apparent Ir depletions are most clearly observed for subaerially erupted Mauna Loa samples (ML 1868-9, R128-0.45, SR0036-1.22 and SR0040-1.07).

5.1.3. HSE characteristics of the parental melt

Removal and accumulation of olivine (and/or co-precipitated phases) have been shown to cause major effects on the absolute and relative abundances of HSE in mafic and ultramafic systems (Barnes et al., 1985; Brügmann et al., 1987; Rehkamper et al., 1999; Puchtel and Humayun, 2001; Bockrath et al., 2004; Maier and Barnes, 2004; Ballhaus et al., 2006). The effects of crystal-liquid fractionation processes are evident in plots of HSE abundances versus MgO for each volcanic center in the Hawaiian suite (Fig. 2). For those plots which show generally linear trends of HSE versus MgO, linear regression of the trends provides a means for estimating the HSE composition of the parental melt for each volcanic center. The intersections of the trends with the estimated parental melt composition of 16 wt.% MgO are used to define the primary HSE abundances of the parental melts (Fig. 6; Table 5). Osmium, Ir, Ru and

Table 3
HSE and $^{187}Os/^{188}Os$ data for Hawaiian picrites

Volcano	Sample Name	Os (ppb)	Ir	Ru	Pt	Pd	Re	$^{187}Os/^{188}Os$
Mauna Kea								
	MK-1-6[d]	0.736	0.476	1.444	1.254	1.572	0.353	0.12924
HSDP-1	R189-8.5B	1.240	0.494	1.787	1.217	1.588	0.046	0.12950
	R197-0.8B	1.089	0.442	1.570	1.039	1.310	0.083	0.12973
	R215-7.2B	0.893	0.456	1.843	1.265	1.189	0.076	0.12947
HSDP-2	SR0129-5.20[c]	0.026	0.193	0.067	1.569	1.383	0.318	0.12987
	SR0328-3.10	1.225	0.483	1.657	1.853	1.753	0.092	0.12970
	SR0346-5.60	0.411	0.301	0.912	1.402	1.487	0.128	0.12919
	SR0401-2.85	1.431	0.648	1.981	1.463	1.146	0.087	0.13073
	SR0450-3.55	1.240	0.781	1.746	1.977	2.386	0.256	0.12865
	SR0502-4.85	1.087	0.681	1.675	1.876	2.498	0.258	0.12920
	SR0683-5.75	1.005					0.262	0.12988
	SR0714-11.55[c]	0.152					0.679	0.12958
	SR0720-18.25	0.519	0.368	1.079	2.494	2.790	0.354	0.13053
	SR0741-7.90	0.241	0.133	0.481	1.004	1.149	0.407	0.12975
	SR0750-12.45	0.405					0.613	0.13032
	SR0756-13.25	1.493					0.467	0.12945
	SR0762-4.60	0.361					0.352	0.13056
	SR0846-2.80[c]	0.325					0.467	0.12982
	SR0891-15.10[d]	1.645	0.814	1.691	3.397	3.899	0.702	0.12987
	SR0940-18.35[d]	0.295	0.268	0.382	0.548	0.488	0.871	0.12951
	SR0954-8.00[d]	0.567	0.352	1.129	2.041	2.836	0.851	0.12870
	SR0964-4.30[d]	1.349	0.752	2.118	2.487	2.627	0.646	0.13067
Mauna Loa								
	ML-2-50[d]	0.902	0.515	1.474	2.373	1.426	0.324	0.13419
	ML-2-50 dup[d]	0.907	0.452	1.298	2.279	1.480	0.323	0.13457
	ML KAH-1	1.263	0.639	1.706	2.886	0.711	0.191	0.13395
	ML 1868-9	0.701	0.365	1.327	1.629	2.498	0.230	0.13491
HSDP-1	R128-0.45	1.320	0.374	1.459	1.690	1.020	0.075	0.13406
HSDP-2	SR0036-1.22	0.656	0.277	0.882	1.973	2.901	0.237	0.13442
	SR0040-1.07	1.138	0.513	1.528	2.956	3.473	0.171	0.13455
	SR0066-0.00	3.013	0.781	2.303	2.333	2.189	0.149	0.13358
	SR0098-2.00	0.873	0.470	1.555	2.154	1.990	0.152	0.13310
	SR0117-4.00	4.424	0.707	1.471	3.377	2.025	0.402	0.13377
Hualalai[d]								
	H-2	0.910	0.423	1.007	1.120	1.228	0.542	0.13685
	H-5	1.421	0.625	1.330	2.673	3.427	0.459	0.13413
	H-7[c]	0.792	0.402	0.876	2.810	3.659	0.769	0.13655
	H-9[c]	0.598	0.429	0.796	2.538	2.470	0.567	0.13624
	H-11	0.935	0.447	0.984	2.805	2.854	0.460	0.13425
	H-23	1.520	0.803	2.586	2.224	2.095	0.202	0.13472
	H-27	1.262	0.550	1.359	1.834	1.647	0.321	0.13437
	H-27 dup	1.144	0.493	1.517	1.786	1.244	0.308	0.13493
	H-P	1.201	0.548	1.823	1.359	2.090	0.174	0.13379
Loihi[d]								
	LO-02-02	0.984	0.836	1.689	5.825	7.301	0.679	0.13518
	LO-02-04	1.150	1.006	1.649	6.526	2.288	0.567	0.13377
	158-9	0.832	0.628	1.244	7.637	7.160	0.721	0.13336
	186-5	0.543	0.470	0.734	5.996	3.220	0.988	0.13102
	186-11	0.173	0.205	0.278	1.500	0.909	1.349	0.13569
	186-11 dup	0.182	0.211	0.281	1.753	0.949	1.338	0.13543
	187-1	1.212	0.879	1.827	6.068	5.863	0.674	0.13062
Kilauea								
	KIL-1-18[d]	0.572	0.558	0.991	2.564	1.672	0.813	0.13113
	KIL-1-18 dup[d]	0.574	0.454	0.995	2.579	1.667	0.824	0.13071
	KIL-2-3[d]	1.007	0.431	1.412	1.101	2.765	0.212	0.13139
	KIL-2-4[d]	0.827	0.439	1.613	1.733	5.882	0.361	0.13149
	KIL-3-1[d]	0.733	0.434	1.182	1.975	2.128	0.215	0.13031
	KIL 1840-2	1.129	0.373	0.984	1.807	2.384	0.171	0.13086
Koolau								
	K 98-08	0.800	0.440	1.156	0.640	0.541	0.216	0.13175
	S497-6[d]	1.124	0.582	1.714	2.618	1.599	0.108	0.13574
	S500-5B[d]	0.950	0.756	2.008	8.634	2.269	0.185	0.26209
	S500-5B dup[d]	0.940	0.657	2.074	8.652	2.168	0.198	0.26139
Kohala[d]								
	KO-1-10	0.368	0.373	0.651	2.219	2.425	0.261	0.13323
	KO-1-20[c]	0.358	0.160	0.356	1.695	1.695	0.392	0.14310
	KOH-1-28	1.052	0.376	1.321	1.929	1.896	0.282	0.13294
	KOH-1-28 dup	0.855	0.362	1.265	1.980	1.917	0.262	0.13310
Lanai								
	LWAW-4	0.827	0.522	1.129	4.171	2.281	0.236	0.13843
	LWAW-7[c]	0.349	0.344	0.568	4.234	2.701	0.221	0.13760
Molokai[d]								
	S501-2	1.857	0.792	2.672	3.383	4.033	0.229	0.13158

Table 3 *(continued)*

Volcano	Sample Name	Os (ppb)	Ir	Ru	Pt	Pd	Re	$^{187}Os/^{188}Os$
PUM								
	PUM[a]	3.9	3.5	7	7.6	7.1	0.35	0.1296
CI Chondrite								
	Orgueil[b]	459	456	650	859	563	38	0.1270

[a] Becker et al., 2006.
[b] Horan et al., 2003.
[c] tholeiitic basalt (MgO <13 wt.%).
[d] submarine sample.

Re contents of the parental melts were estimated in this manner for all volcanic centers from which greater than three samples were collected. Platinum and Pd exhibited much more scatter on the HSE versus MgO plots, so the parental melt composition for these two elements was not estimated for all volcanic centers. Platinum contents were estimated for Mauna Kea, Mauna Loa, Hualalai and Kilauea; whereas, Pd contents, which exhibited the most scatter on the HSE versus MgO plots, were estimated only for Hualalai and Kilauea. Samples with nearly 16 wt.% MgO and that are also in equilibrium with associated olivines approximate parental melt compositions, as discussed above. The HSE data for these samples (H-2, H-5, H-9, H-11, H-27, Lo 158-9 and Kil 1-18) tend to cluster close to the linear regression lines, consistent with our approach.

The estimated parental melt HSE abundances (where possible) for all volcanic centers are generally similar (Fig. 7). Osmium, Ir, Ru and Re abundances in the majority of parental melts are 0.5±0.2 ppb, 0.45±0.05 ppb, 1.2±0.2 ppb and 0.35±0.05 ppb respectively. Likewise, estimated Pt abundances in the parental melt are similar at 2.3±0.2 ppb. Notable exceptions include the estimated Os content of the Hualalai parental melt, which is higher at 1.0 ppb. The parental melt for Loihi is estimated to have the lowest abundances of Os, Ir and Ru, as well as the highest Re content (1.2 ppb). Although linear trends between Pt and Pd with MgO were not observed, Loihi picrites also have strong enrichments in these elements.

5.1.4. Estimated bulk distribution coefficients

For those elements that show good linear correlations with MgO, linear regressions of the trends can also be used to estimate bulk solid/melt partition coefficients (i.e. D values; Puchtel and Humayun, 2001). To do this, the linear HSE-MgO trends were extrapolated to the average MgO content of co-precipitating olivine for each shield volcano, the primary Mg-containing liquidus phase. This permits estimation of the bulk concentration of the HSE in the co-precipitating solid phases (i.e., olivine, chromite; Table 5; Fig. 6). The HSE concentrations calculated in the solid (olivine) were then related to those of the parental melts to obtain *D* values. Estimated *D* values for Os (2.2 to 7.1), Ir (1.2 to 5.6) and Ru (2.5 to 6.3) indicate that these elements all behaved compatibly in the picrites from each volcanic center. The estimated *D* values for Pt (0.2 to 0.7) indicate that it behaved incompatibly. Palladium does not display a meaningful linear correlation with MgO in any of the volcanic centers, indicating that olivine fractionation may have had little control on Pd. These *D* values compare favorably to other studies of HSE in high MgO Hawaiian rocks from Kohala (Jamais et al., 2008) and Kilauea Iki Lava Lake (Pitcher et al., in press).

For Hawaiian picrites, we conclude that Os, Ir and Ru behaved compatibly, during crystal-liquid fractionation with their abundances directly related to the amount of olivine present. It is likely, however, that these elements are sited in chromite and sulfide inclusions present within the olivine grains, rather than structurally bound within the olivine (Yi et al., 2000; Puchtel and Humayun, 2001; Brenan et al., 2003, 2005). Platinum, Pd and Re behaved incompatibly and are evidently contained primarily in the matrix phases.

5.2. Additional processes potentially affecting HSE in parental melts

5.2.1. Crustal assimilation

Assimilation of crustal material by mantle-derived magmas as they ascend through the oceanic crust has the potential to alter the HSE characteristics and Os isotopic composition of a melt (Martin et al., 1994; Marcantonio et al., 1995; Roy-Barman and Allégre, 1995; Widom and Shirey, 1996; Lassiter and Hauri, 1998; Yi et al., 2000; Gaffney et al., 2005; Bizimis et al., 2007). Oceanic crust tends to have high Re/

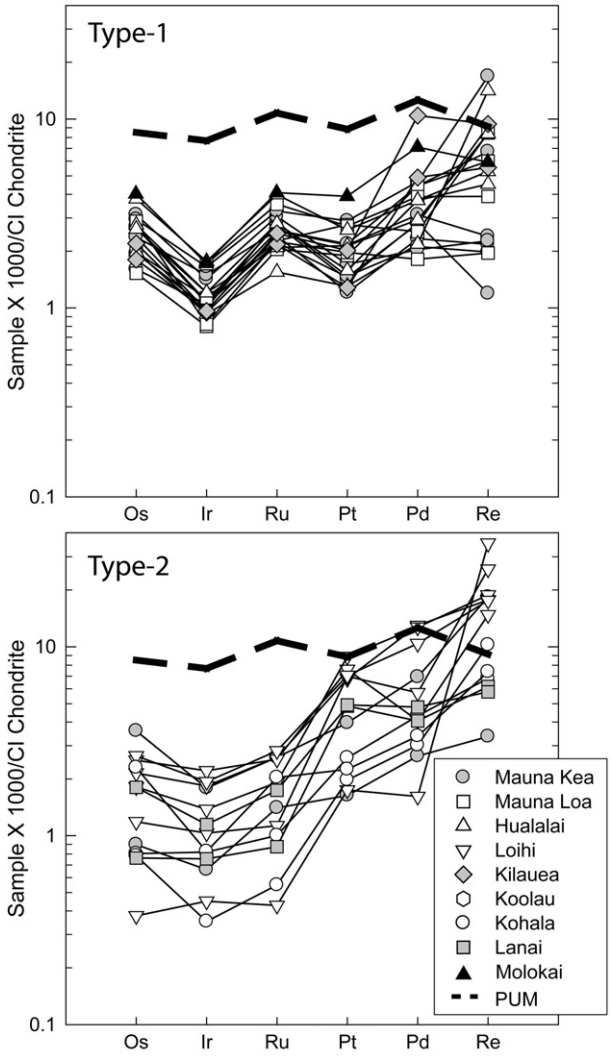

Fig. 1. HSE patterns for the Hawaiian picrites. Type-1 picrites differ from Type-2 in having lower Pd/Ir and Pt/Ir ratios. Type-1 picrites also tend to have higher Os/Ir and Ru/Ir ratios. PUM is thought to be representative of fertile peridotites, prior to the removal of material from the upper mantle (Becker et al., 2006).

Os ratios due to the differences in compatibility between Re and Os during mantle melting. Over time, this leads to the development of highly radiogenic $^{187}Os/^{188}Os$ ratios. Assimilation of highly radiogenic oceanic crust by a picritic melt may, thus, result in an increase in $^{187}Os/^{188}Os$. This effect can be highly significant for basaltic melts with very low Os contents, or during the late stages of shield-building.

For Hawaiian shield volcanoes, assimilation of oceanic crust has been suggested for late shield-stage lavas from West Maui (Gaffney et al., 2005) as well as for samples from Mauna Kea (Lassiter and Hauri, 1998) and Haleakala (Martin et al., 1994) to explain radiogenic $^{187}Os/^{188}Os$ ratios. However, bulk oceanic crust contains much lower absolute abundances of the HSE (except Re) than the picrites analyzed in the present study (Peuker-Ehrenbrink et al., 2003). Bulk assimilation of the oceanic crust should, therefore, result in lower abundances of the HSE.

To quantitatively examine this possibility we consider the effects of bulk assimilation by modeling the addition of ~100 Ma Pacific oceanic crust that underlies Hawaii ($^{187}Os/^{188}Os$=0.9; Os=0.02 ppb; Re=1.5 ppb; Ir=0.009 ppb; Ru=0.03 ppb; Pt=0.3 ppb and Pd=0.3 ppb; Tatsumi et al., 1999; Peuker-Ehrenbrink et al., 2003) to a representative parental melt for the Hawaiian picrites. The Kilauea parental melt was chosen for the Hawaiian picrite end-member because it has the least radiogenic $^{187}Os/^{188}Os$ ratios (0.130) and has typical HSE abundances for Hawaiian picrites (Os=0.7 ppb; Re=0.4 ppb; Ir=0.4 ppb; Ru=1.1 ppb; Pt=2.0 ppb and Pd=1.5 ppb).

Calculations show that simple mixing of 1% to 20% proportions of a crustal assimilant similar to a Kilauea-like parental melt would have a limited, mostly dilutional effect, on the concentrations and relative abundances of the HSE in a picrite parental melt. For example, addition of 20% of oceanic crust would result in a decrease in Os, Ir, Ru, Pt and Pd abundances of ~19%. At the same time, Re would be enriched by ~30% (Fig. 8) and $^{187}Os/^{188}Os$ ratios would be raised by ~4% (0.130 to 0.135). Such large amounts of assimilation, however, are inconsistent with the major element compositions of the picrites, because the addition of large amounts of basaltic material to a picritic melt would dilute the MgO content such that the melt would no longer be picritic and would likely result in equilibration with olivine of different composition than Fo_{90}. Additions of more geologically feasible proportions of <5% would not be resolvable within the variations present in the HSE abundance data. In a hypothetical mixture of the Kilauea parental melt with 5% crustal contamination, the $^{187}Os/^{188}Os$

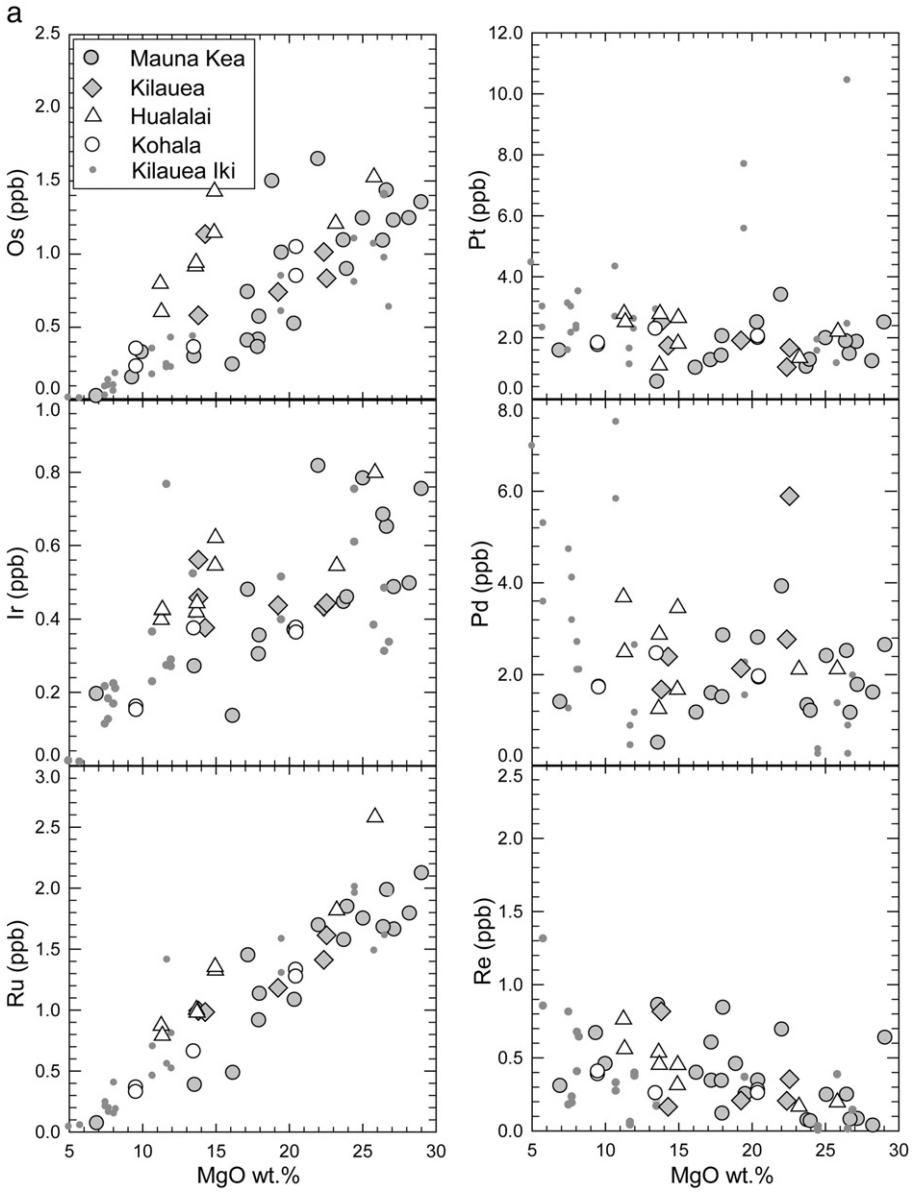

Fig. 2. a–b): HSE-MgO trends for all volcanoes analyzed in this study. Small gray symbols are from Kilauea Iki Lava Lake (Pitcher et al., in press).

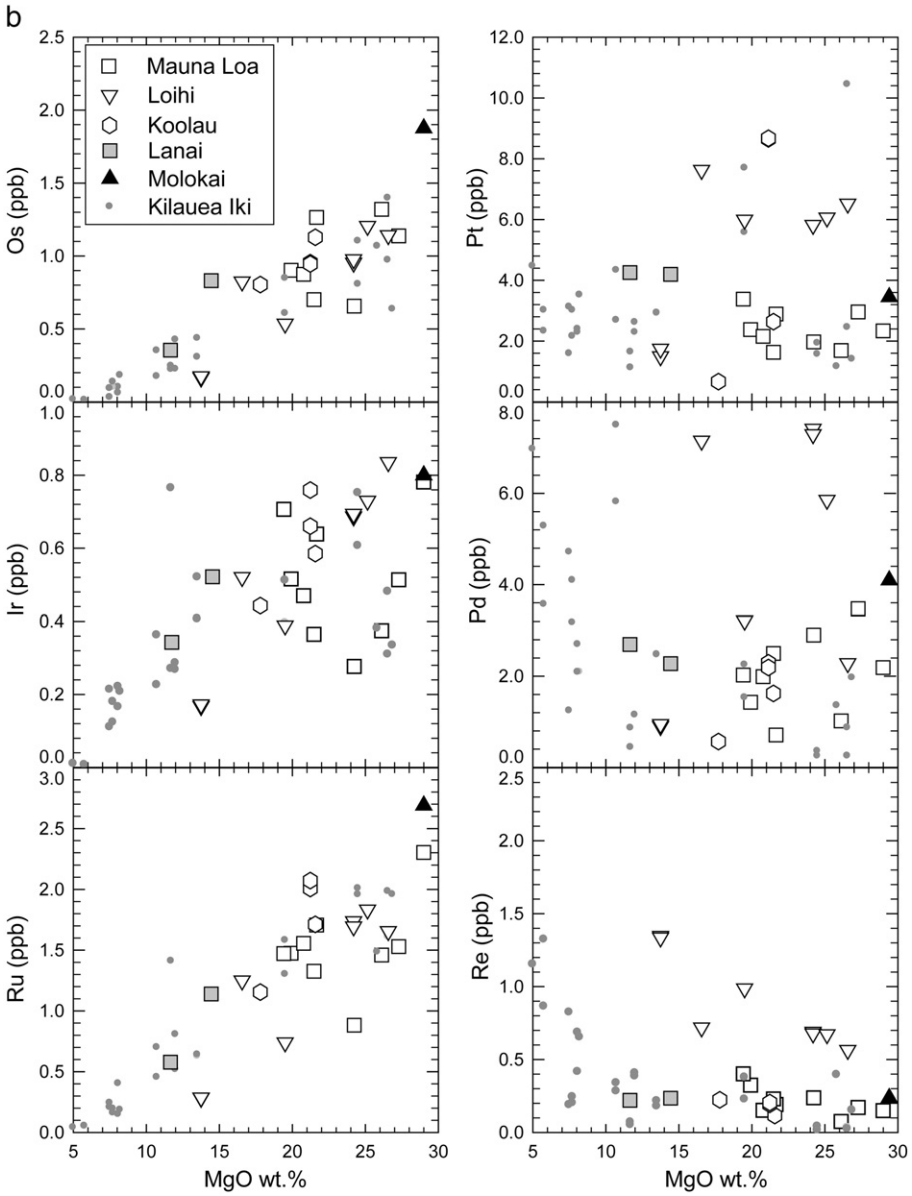

Fig. 2 (*continued*).

ratio of the resulting melt would increase by only ~1%. Once again, this limited effect would not be resolvable in Os isotopic data for Kilauea. The limited variation in $^{187}Os/^{188}Os$ within volcanic centers suggests that variable amounts of bulk assimilation had little effect on the Os isotopic composition and HSE abundances in the picritic suite.

If crustal sulfide could be selectively assimilated by the picritic magmas during transport through the crust, as opposed to bulk assimilation, the HSE budget of the rising magma might be changed without having a significant effect on the major element composition. For example, Yi et al. (2000) suggested that the sulfides present in Loihi picrites (including sample Lo-187-1) may represent assimilated crustal sulfide, as well as sulfide that co-precipitated with olivine during olivine accumulation. However, the similar HSE patterns and narrow range in $^{187}Os/^{188}Os$ ratios found for each shield volcano (Figs. 1 and 3) argue against variable crustal sulfide assimilation being a major process for Hawaiian picrites. Crustal sulfides are likely to be highly variable in composition, possessing a wide range in HSE abundances and varying Re/Os ratios (Peuker-Ehrenbrink et al., 2003). The range of Re/Os ratios, coupled with different residence times within the crust, would lead to a broad range in $^{187}Os/^{188}Os$ ratios. Given the variability in these crustal sulfides, it would be unlikely for samples from the same volcanic center to inherit such similar HSE patterns and $^{187}Os/^{188}Os$ ratios. We conclude that assimilation of sulfides is unlikely to have significantly affected the HSE abundances in these rocks. However, it is a process worth further investigation, especially via analysis of S isotopes.

5.2.2. Fe–Mn crust contamination

The addition of Fe–Mn rich materials, including crusts, umbers and nodules, into mafic magmas have been suggested as a potential means to affect the HSE and Os isotopic characteristics of putative plume-derived magmas, as these materials tend to scavenge HSE, particularly Pt, from seawater (Smith, 2003; Baker and Jensen, 2004; Schersten et al., 2004). Previous studies have argued that these materials can be recycled into the mantle sources of plumes during the subduction process. Here we examine the affect of Fe–Mn contamination of a sample on the seafloor.

Sample S500-5B permits examination of the effects that Fe–Mn alteration can have on HSE abundances in the picrites. The Mn content of our piece of S500-5B is 1.62 wt.%, compared to a maximum of 0.18 wt.% for all other samples (Table 1). The high Mn concentration of this sample

indicates incorporation of ~5% of Mn-crust material (Mn=25 wt.%; Schersten et al., 2004). The absolute and relative abundances of Os, Ir, Ru, Pd and Re are similar to other Hawaiian picrites, and do not appear to be affected by major Mn deposition. A significant enrichment is observed for Pt, however, consistent with its addition during the alteration (Fig. 9). Further, the alteration was evidently also accompanied by a dramatic increase in the $^{187}Os/^{188}Os$ ratio of the sample (0.260). Although seafloor alteration, resulting in the addition of Mn-rich materials to the picrites, can evidently cause Pt enrichment and an increase in $^{187}Os/^{188}Os$, it appears to have had no effect on the other HSE and on the remaining samples which have normal Mn contents.

Of all of the picritic suites studied here, only samples from Loihi show appreciable enrichments in Pt abundances, with up to three times more Pt (average=6.4 ppb) than picrites from other volcanic centers (average=2.0 ppb). Loihi picrites, however, also have elevated Pd and Re abundances, as well as low Mn abundances (0.17 to 0.19 wt.%). Consequently, we conclude that the Pt enrichment was not caused by seafloor alteration or the presence of recycled seafloor precipitates in their mantle source.

5.2.3. Effects of partial melting and crystal-liquid fractionation

Partial melting can cause significant HSE fractionation (Barnes et al., 1985; Barnes and Picard, 1993; Shirey and Walker, 1998; Rehkamper et al., 1999; Momme et al., 2003; Bockrath et al., 2004; Maier and Barnes, 2004; Pearson et al., 2004). The effects of partial melting can most clearly be observed by a comparison between the HSE content of a high degree partial melt, such as some komatiites (Puchtel et al., 2004; Puchtel and Humayun, 2005), and a lower degree melt, such as a typical MORB (Tatsumi et al., 1999; Peuker-Ehrenbrink et al., 2003).

The HSE abundances of a primary mantle melt are primarily controlled by the presence or absence of trace phases in the melt residue. Sulfides, in particular, are important carriers of the HSE in the mantle, although the IPGE (Os, Ir and Ru) are also hosted by other phases including Os-Ir-Ru alloys (Maier et al., 2003; Bockrath et al., 2004; Ballhaus et al., 2006; Luguet et al., 2007). The IPGE are typically incorporated into Mss (mono-sulfide solid solution), which is frequently included in silicate phases (Maier et al., 2003; Bockrath et al., 2004; Ballhaus et al., 2006; Luguet et al., 2007). The PPGE (Pt and Pd) are commonly hosted by Cu-sulfides which are usually found as interstitial phases (Maier and Barnes, 2004). Rhenium, on the other hand, is not evidently controlled by this inter-sulfide partitioning. It typically remains moderately incompatible during mantle melting and may be controlled by silicate partitioning. Thus, a strong Re enrichment is a common feature of most mantle-derived melts (e.g., Tatsumi et al., 1999; Peuker-Ehrenbrink et al., 2003).

Higher degree partial melts (>20%), such as some komatiites, are commonly S-undersaturated. Consequently the HSE can be efficiently removed from the source, as the hosting sulfides are entirely incorporated into the melt. Such melts tend to have relatively flat chondrite-normalized HSE patterns (approaching chondritic Pd/Ir ratios), as well as higher absolute abundances of these elements, relative to other mafic melts (Puchtel et al., 2004; Puchtel and Humayun, 2005). Conversely, lower degree partial melts (<20%), such as most basalts, tend to be S-saturated, resulting in incomplete dissolution of sulfide in the mantle source. In these cases the PPGE can be effectively fractionated from the IPGE as the interstitial Cu-rich sulfides melt out before Mss, resulting in magmas with high Pd/Ir ratios. In a similar manner, incongruent melting of mixed sulfide phases may also result in a residue containing Mss (Maier and Barnes, 2004; Ballhaus et al., 2006).

The picritic samples analyzed in this study have estimated parental melt concentrations of the HSE that fall between those of komatiites and Pacific MORB (Fig. 7). Norman and Garcia (1999) concluded that the degree of partial melting necessary to generate the Hawaiian picrites was ~4 to 10%, indicating that these samples were sulfur-saturated at the time of melting. However, as a melt ascends, sulfide can be eliminated by decompression causing the melt to become sulfur-undersaturated (Ballhaus et al., 2006). Although these picrites represent similar degrees of partial melting as MORB, the difference in HSE abundances might be attributed to late-stage sulfide fractionation processes. MORB are generally much more evolved than OIB, and have, therefore, lost HSE due to sulfide fractionation (Ballhaus et al., 2006). The partial melting estimates were used by Bennett et al. (2000) to argue for the presence of variable amounts of residual sulfide in the Hawaiian plume source. These authors postulated that the observed variations in the HSE abundances likely did not reflect large differences in the HSE composition of the source regions of the volcanoes, but rather the presence of variable proportions of residual sulfides in the mantle sources of each volcanic center. For a given mantle source, lower degrees of partial melting may result in larger amounts of residual sulfide, which would lead to lower absolute abundances of the HSE in the resulting melt. The HSE patterns of the picrites analyzed by Bennett et al. (2000) are similar to the Type-2 pattern observed in the present study. Samples with Type-2 patterns tend to have higher average abundances of Pt and Pd than samples with Type-1 patterns, resulting in elevated Pd/Ir and Pt/Ir ratios. We note that these two pattern types are observed within a single

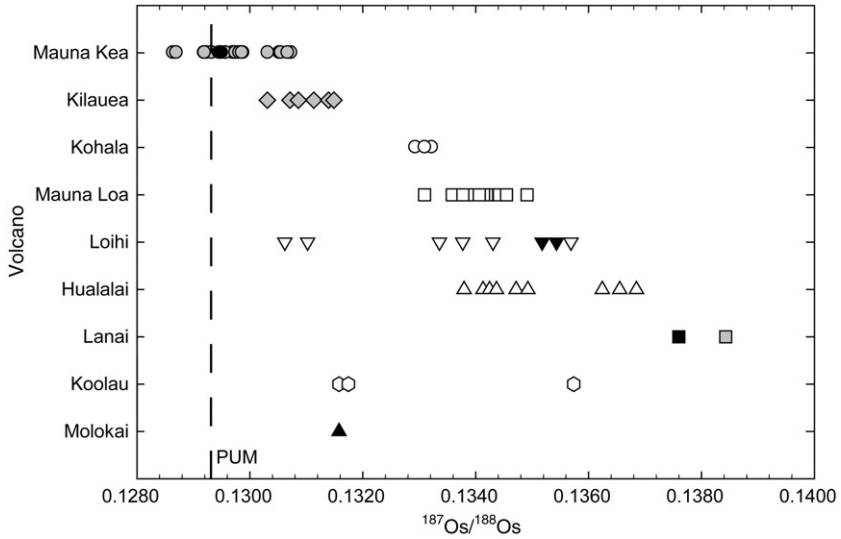

Fig. 3. Range of $^{187}Os/^{188}Os$ ratios for each volcanic center. Mauna Kea and Kilauea are characterized by lower $^{187}Os/^{188}Os$ ratios, whereas Mauna Loa, Loihi and Hualalai are more radiogenic. Black symbols denote tholeiitic basalts (MgO <13 wt.%). Error bars for $^{187}Os/^{188}Os$ ratios are approximately the same size as the symbol. PUM estimate is from Meisel et al. (2001).

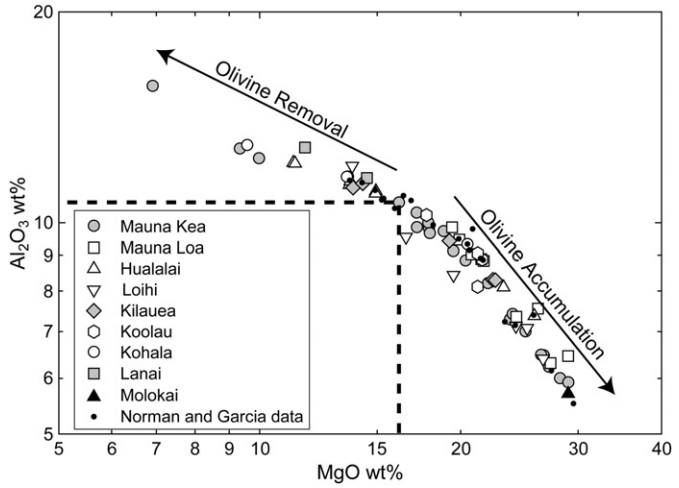

Fig. 4. Log–Log variation diagram of Al_2O_3 vs. MgO. The break in slope at ~16 wt.% MgO and ~11 wt.% Al_2O_3 marks the estimated parental melt composition. Samples with >16 wt.% MgO are presumed to have accumulated olivine, whereas samples with <16 wt.% MgO have had olivine removed. Small black symbols are samples from Norman and Garcia (1999).

volcanic center and are not correlated with MgO content (i.e. samples with similar MgO contents can exhibit either pattern). If the Type-2 samples result from lower degrees of partial melting, the source region may retain more of the PPGE-hosting interstitial Cu-rich sulfide relative to the Type-1 samples. Thus, if the difference between the two HSE patterns is due to significant differences in the degree of partial melting, it should be reflected in the ratios of trace elements that would be sensitive to this process (e.g., La/Yb, Rb/Sr), as well as in the MgO content of the parental melts (Norman and Garcia, 1999). However, with the exception of Loihi, there is no discernible difference between the two HSE trends in terms of incompatible element ratios indicative of partial melting (Fig. 10).

Slight differences in the degree of partial melting, however, may account for some of the inter-volcano differences. Samples from Loihi possess higher abundances of Pt, Pd and Re than the other volcanic

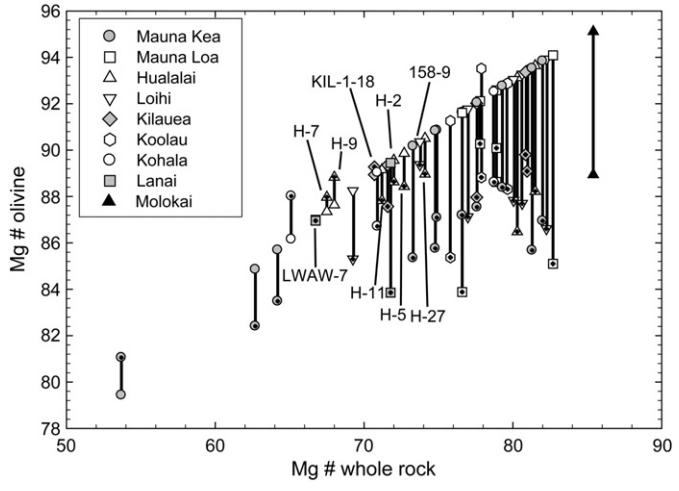

Fig. 5. A plot comparing measured olivine Mg# (crossed symbols) to the calculated Mg# of olivine in equilibrium with the whole rock (open symbols). Samples that have measured olivine that is close to equilibrium with the whole rock may approximate the parental melt composition for the picrites. Samples that have a whole rock composition that is in equilibrium with included olivine phenocrysts are H-2, H-5, H-7, H-9, H-11, H-27, Lo 158-9, Kil 1-18 and LWAW-7. Large deviations between the Mg# of the measured and calculated olivine denote those samples whose whole rock composition is not in equilibrium with olivine present in the sample. These samples have experienced variable amounts of olivine removal or accumulation.

Table 4
Estimated percentages of olivine removal and accumulation

Volcano	Number of samples	MgO low	MgO high	Maximum removal	Maximum Aaccumulation
Mauna Kea	22	6.93	29.07	37.1	26.7
Mauna Loa	9	19.42	28.99	n/a	26.5
Hualalai	8	11.23	25.8	10.6	20.0
Loihi	6	13.76	26.58	8.3	21.6
Kilauea	5	13.80	22.55	4.9	13.4
Koolau	3	17.78	21.55	n/a	11.3
Kohala	3	9.60	20.52	14.2	9.2
Lanai	2	11.69	14.48	12.5	n/a
Molokai	1	28.96	28.96	n/a	26.5

centers. Norman and Garcia (1999) inferred from trace element modeling that Loihi magmas formed from the lowest degrees of partial melting among the Hawaiian volcanoes. This interpretation is supported by the present study, as Loihi has the highest concentrations of the more incompatible PPGE, as well as the highest La/Yb ratios in the sample suite. Differing degrees of partial melting can also have a bearing on the absolute abundances of the HSE in the sample suite, based on the proportion of residual sulfide that may be left in the mantle. However, this process alone may not produce the variations in relative abundances that are observed between Type-1 and Type-2 HSE patterns.

By process of elimination, we speculate that the variations between Type-1 and Type-2 samples mainly relate to slight differences in the degree of partial melting and the sulfide mineralogy of the residual mantle, coupled with minor dissimilarities in the crystal-liquid fractionation process for each volcanic suite. This hypothesis may be best observed in samples H-2 (Type-1 HSE pattern) and H-11 (Type-2 HSE pattern) from Hualalai, both of which contain ~13.6 wt.% MgO and have olivine in equilibrium with the whole rock. These samples are from the same volcanic center and have similar La/Yb ratios, so they likely do not reflect a change in the degree of partial melting. The different HSE patterns instead most probably reflect minor differences in the crystal-liquid fractionation process, which could result from slightly different

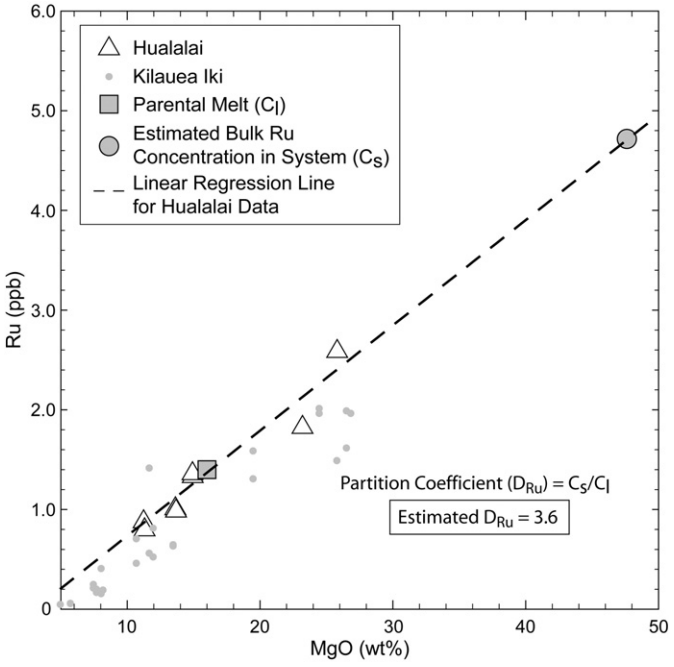

Fig. 6. Example for how the HSE content in a parental melt and the partition coefficient were estimated, using Ru abundances from Hualalai. The parental melt is assumed to contain 16 wt.% MgO, and its Ru abundance is determined by the linear regression of the data. To estimate the partition coefficient, the linear regression line was extrapolated to the MgO content of co-existing olivine. This MgO content is presumed to give the bulk HSE concentration present in the crystal phases.

Table 5
Estimated bulk partition coefficients and HSE abundances in picritic parental melts

Volcano		Ni	Os	Ir	Ru	Pt	Pd	Re	Average $^{187}Os/^{188}Os$	Re/Os	Pt/Os
Mauna Kea	parental melt	688	0.50	0.41	1.14	2.20	–	0.40	0.1297	0.80	4.40
	2σ		0.03	0.09	0.13	0.45	–	0.02		0.04	0.65
	D	4.1	5.4	2.3	2.8	–	–	–			
Mauna Loa	parental melt	416	0.73	0.48	1.20	2.55	–	0.40	0.1341	0.55	3.50
	2σ		0.17	0.11	0.16	0.33	–	0.04		0.13	0.81
	D	7.5	2.6	1.3	2.5	0.7	–	–			
Hualalai	parental melt	782	1.00	0.50	1.40	2.20	2.20	0.40	0.1351	0.40	2.20
	2σ		0.01	0.00	0.01	0.03	0.04	0.04		0.05	0.40
	D	3.9	2.2	2.2	3.4	0.2	–	–			
Loihi	parental melt	728	0.44	0.38	0.66	–	–	1.20	0.1336	2.74	–
	2σ		0.07	0.04	0.12	–	–	0.07		0.45	–
	D	3.1	6.3	5.6	6.3	–	–	–			
Kilauea	parental melt	754	0.65	0.42	1.10	2.13	2.20	0.40	0.1310	0.61	3.28
	2σ		0.07	0.02	0.03	0.11	0.36	0.08		0.12	0.28
	D	4.7	2.9	1.2	2.7	–	–	–			
Koolau	parental melt	665	0.52	0.48	1.17	–	–	0.30	0.1337	0.57	–
	2σ		0.13	0.12	0.31	–	–	0.03		0.11	–
	D	4.5	7.1	2.8	4.4	–	–	–			

magma evolution histories. Chromite fractionation in a PGE-chromite saturated (but sulfide-undersaturated) melt may result in the direct removal of the IPGE as a magma ascends, as chromite may act as a nucleation point for IPGE alloys (Ballhaus et al., 2006). This process can further fractionate the IPGE from the PPGE, as a magma ascends through the mantle or as a magma sits in a high level magma chamber. Removal of Mss from an immiscible sulfide liquid could also fractionate the IPGE from the PPGE. We speculate that sample H-11 lost Os, Ir and Ru relative to Pt and Pd due to the direct removal of IPGE phases (i.e. Mss or chromite-associated IPGE alloys) during magma ascent or through the removal of cumulate phases in a higher-level magma chamber. The retention of chromite-associated IPGE alloys could also potentially explain the reproducibility of the Os-Ir-Ru relative abundances observed in the Type-1 HSE pattern.

5.3. Source heterogeneities

In order to account for variations in $^{187}Os/^{188}Os$ ratios, a parameter not affected by crystal-liquid fractionation or variable partial melting, some level of HSE heterogeneity must be present in the Hawaiian mantle plume. These isotopic variations require long-term differences in the Re/Os ratios of the source regions for the Hawaiian volcanic centers (Lassiter and Hauri, 1998; Brandon et al., 1999; Bennett et al., 2000; Bryce et al., 2005). Previous authors have attributed the $^{187}Os/^{188}Os$ variations to the presence of recycled oceanic mafic crust and/or sediments in the plume source for Hawaiian volcanoes (e.g., Lassiter and Hauri, 1998). A role for core-mantle interaction has also been proposed to account for some of the ^{187}Os enrichment (and corresponding ^{186}Os enrichment) observed in some volcanic centers (Brandon et al., 1999).

Currently, precisely extrapolating mantle source HSE abundances from parental melt compositions is impossible because of the compatible to slightly incompatible nature of these elements. However, given similar melting conditions, the assumption can be made that large scale variations in absolute and relative HSE abundances in the mantle sources would be reflected in the parental melt compositions.

Relative and absolute HSE abundances in the picrites show no correlation with variations in $^{187}Os/^{188}Os$ ratios (Fig. 11), suggesting either insufficient resolution, or that relatively recent processes have led to a decoupling between these geochemical parameters. To consider the required level of resolution necessary, we use the mixing model of Lassiter and Hauri (1998). They concluded that the addition of ~30% of 1.8 Ga recycled oceanic crust, comprising a mixture of 97% basalt and 3% sediment, to the mantle source for the Hawaiian plume could produce the most radiogenic observed basalts ($^{187}Os/^{188}Os$ ratios of 0.148 for Koolau). Following the parameters of their modeling, the Re/Os ratio of their hybrid mantle source would increase by a factor of ~2. If the increased Re/Os ratio of the source is also reflected in the parental melts, it would provide a direct link between the $^{187}Os/^{188}Os$ isotopic composition and the HSE characteristics of the picrites and the source. However, although the Re/Os ratios of the estimated

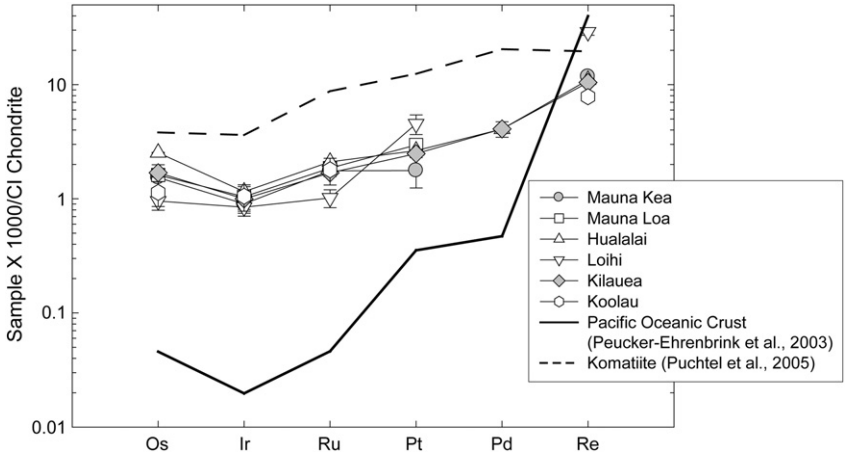

Fig. 7. A chondrite-normalized HSE pattern plot showing the estimated parental melt compositions for all Hawaiian volcanic centers with greater than 3 samples. Also shown are the HSE patterns for a typical MORB (Peuker-Ehrenbrink et al., 2003) and a komatiite (Puchtel and Humayun, 2000, 2005). Note that the HSE abundances for the Hawaiian parental melts are intermediate between a low-degree melt (MORB) and a high-degree melt (komatiite).

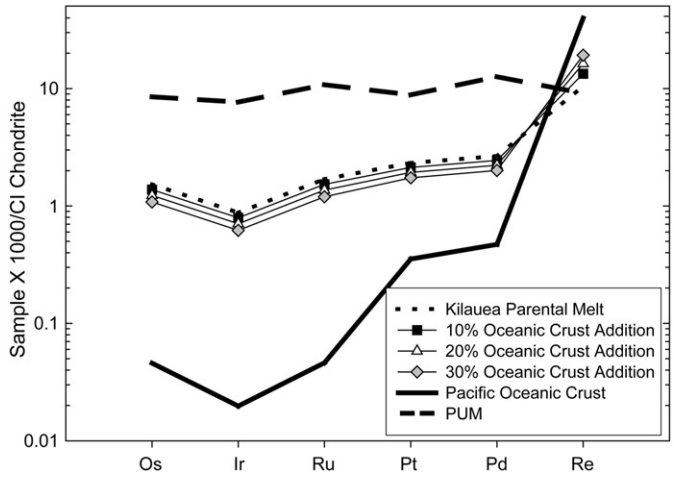

Fig. 8. Example of how differing amounts of crustal contamination can affect the HSE systematics of a sample. Crustal contamination has a diluting effect on absolute HSE abundances, but no effect on relative abundances. Small to large additions (0–20%) of oceanic crust to a magma results in a small decrease in the HSE abundances in the magma, however, crustal material is highly radiogenic, making the addition of large proportions of crust to a magma untenable.

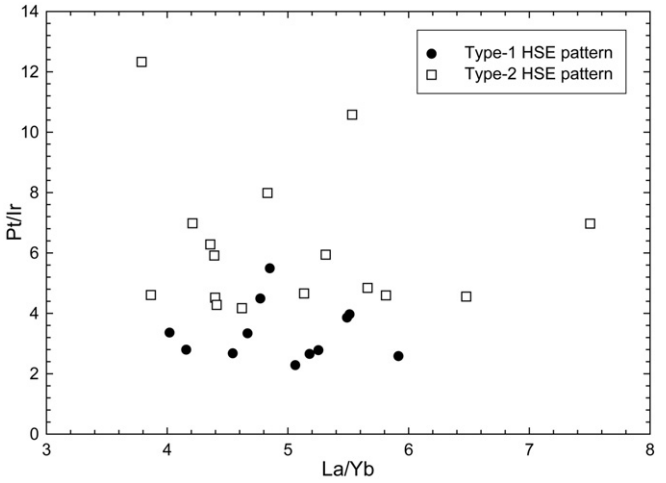

Fig. 10. A plot of Pt/Ir versus La/Yb. La/Yb is a trace element ratio that is not affected by olivine crystallization and varies with the degree of partial melting. If the difference in Pt/Ir ratios between Type-1 and Type-2 HSE patterns was a result of different degrees of partial melting, a relationship between the two ratios would be expected. However, there is no correlation between the HSE patterns and La/Yb which indicates that partial melting was not the cause of the difference. La/Yb data are from Norman and Garcia (1999), Huang and Frey (2003) and Arevalo (pers. comm.).

parental melts in this study also vary by a factor of 2, the variation is in the opposite direction predicted by oceanic crust recycling. For example, the parental melt for Hualalai, which has the highest average $^{187}Os/^{188}Os$ ratio in this suite, is estimated to have the lowest Re/Os ratio; whereas, the estimated parental melt for Mauna Kea has the lowest average $^{187}Os/^{188}Os$ ratio, but the highest Re/Os (Table 5; Fig. 11). This result suggests that either the Re/Os of parental melts do no accurately reflect the Re/Os of the mantle source, or that relatively recent processes have affected the Re/Os ratios of the sources, and caused a decoupling of ^{187}Os and Re/Os.

One clue to the lack of correlation may be the Os enrichment in Hualalai lavas (Fig. 2a). The parental melts for Hualalai have a higher estimated Os abundance (~1.0 ppb) than estimates for the other volcanic centers (0.5±0.2 ppb). This increase in Os abundance is accompanied by estimated Ir and Ru contents that fall on the high end of the Hawaiian spectrum, but not significantly greater than the other estimated parental melts. The enrichment in Os, relative to Ir and Ru, could be the result of melt percolation processes, which have been shown to fractionate Os from the other IPGE.

For example, Büchl et al. (2002, 2004a,b) reported that melt percolation processes occurring in the Troodos Ophiolite on Cyprus, resulted in the fractionation of Os from Ir and Ru. Fractionation occurs as these elements become mobilized, and behave incompatibly, contrary to their behaviour during partial melting processes. Troodos

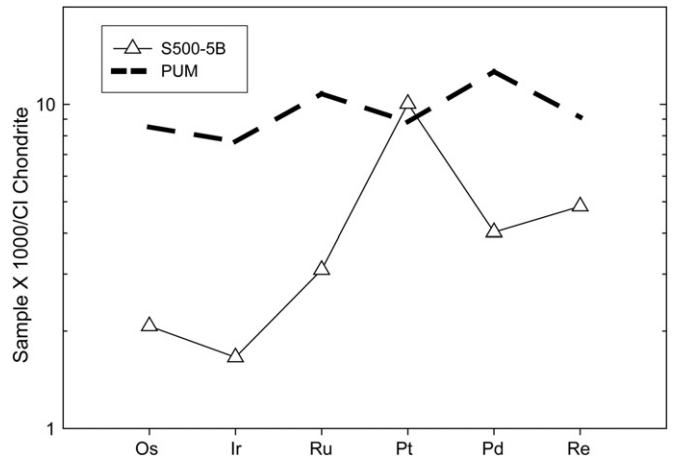

Fig. 9. Sample K500-5B from Koolau, which has been pervasively altered by Mn-rich material. The HSE pattern for this sample is consistent with other volcanic centers, with the exception of Pt, which shows a marked enrichment.

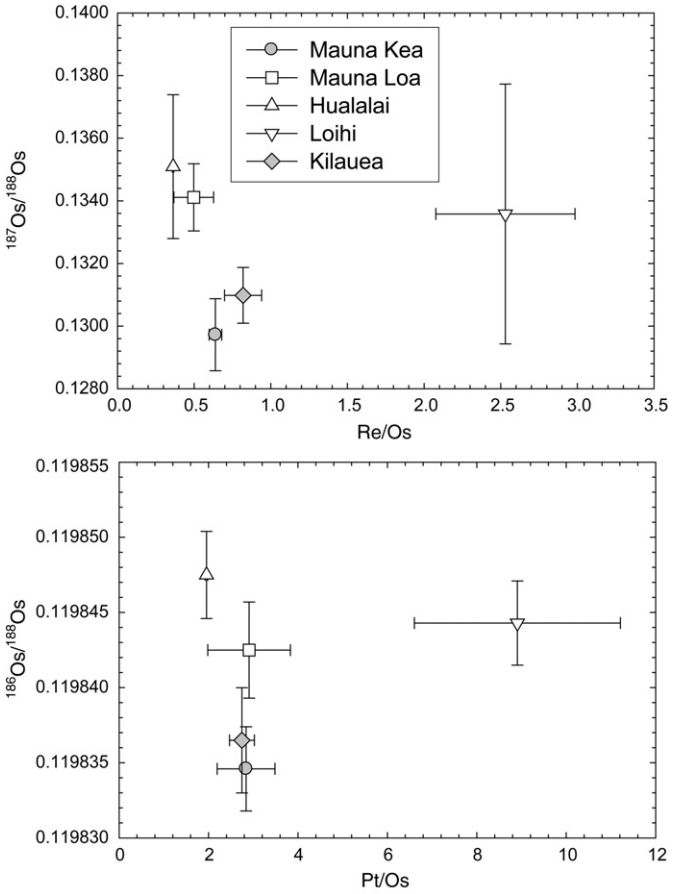

Fig. 11. Plots of Os isotopic composition versus Re/Os and Pt/Os ratios. There is no correlation between these parameters, suggesting that either recent events have modified the Re/Os and Pt/Os characteristics of the mantle sources, or that parental melt HSE abundances are decoupled from those of their mantle source. $^{186}Os/^{188}Os$ data from Brandon et al. (1999).

harzburgite samples, which Büchl et al. (2002) concluded formed by low melt/rock ratios, have higher Os/Ir ratios than associated dunites (high melt/rock ratios). These harzburgites were interpreted to have undergone open-system melting, which resulted in an up to ~6-fold increase in Os/Ir relative to the dunites, yet retained the $^{187}Os/^{188}Os$ ratio of the mantle source. If such a melt percolation process occurred for Hualalai, at low melt/rock ratios, a modified source region with higher Os/Ir and Os/Ru ratios could have been formed. Partial melting of this modified source would result in a parental melt with higher Os/Ir and Os/Ru rations. An added consequence of this style of melt percolation would be a lowering of the Re/Os ratio, which is observed for the estimated Hualalai parental melt (Re/Os=0.4). If the interpretation of this process is correct, the enriched $^{187}Os/^{188}Os$ at Hualalai requires that it was a relatively recent event because the lower Re/Os ratio would ultimately lead to a retardation in the $^{187}Os/^{188}Os$ ratio. However, the high Os/Ir ratios in the harzburgites did not result from enrichments in Os, but rather depletions in Ir.

Becker et al. (2001) documented enriched Os concentrations in pyroxenitic precipitates caused by the melt percolation of a Mg-rich silicate melt through dunite channels from the Bohemian massif. They indicated that the Os budget of the pyroxenite was dominated by Os that was originally derived from mantle peridotite, which provides a means to increase the Os abundance of a melt if this pyroxenitic material can be incorporated into later melting events. Recently, Sobolev et al. (2005, 2007) suggested that recent melt percolation events have occurred in the mantle source region of the Hawaiian plume, resulting in a mixed pyroxenite–peridotite source, which provides a means to decouple HSE abundances and ^{187}Os isotopic compositions of Hawaiian parental melts. At this time, however, it is difficult to assess the effects of the peridotite to pyroxenite conversion on HSE abundances because the partitioning of these elements between these two phases is unknown. Such processing will have to be further examined via experimental techniques.

Some studies have also noted coupled enrichments between both $^{187}Os/^{188}Os$ and $^{186}Os/^{188}Os$ ($^{190}Pt \rightarrow {}^{186}Os + \alpha$; $\lambda = 1.417 \times 10^{-12}$ yr^{-1}) in Hawaiian picrites and komatiites from Gorgona Island (Brandon et al., 1999; Brandon et al., 2003). Recent models attempting to reconcile these data have appealed to mixed pyroxenite–peridotite sources and redistribution of base-metal sulfides (BMS) to explain the co-variations (Bockrath et al., 2004; Ballhaus et al., 2006; Luguet et al., 2008), consistent with claims of a pyroxenitic source for Hawaiian lavas (Sobolev et al., 2005, 2007). Some of these models suggest that peridotitic mantle sources can be hybridized by the addition of melts with high Pt/Os and Re/Os ratios, which are originally derived from subducted oceanic crust. Base-metal sulfides, which concentrate the HSE, may also be transferred into the hybridized source.

To consider this interpretation, we model the addition of ~0.8% of the most radiogenic BMS discussed in the Luguet et al. (2008) study to a peridotite source and assess the effect of this addition on $^{187}Os/^{188}Os$ ratios and HSE abundances. If such a process can physically occur, the resulting hybridized mantle would have an $^{187}Os/^{188}Os$ ratio of ~0.14, consistent with data for Lanai. A consequence of the addition of this sulfide, however, is a substantial increase in the Pt abundance of the mantle source from ~5 ppb to 17 ppb, accompanied by a 3-fold increase in the Pt/Os ratio. The increase in Pt abundances and Pt/Os ratios should be resolvable within the HSE data reported here, assuming that the increase in the source is reflected in the parental melt. This type of Pt enrichment is not observed in the more ^{187}Os or ^{186}Os enriched picrites from Hualalai (Brandon et al., 1999). Moreover, the estimated Pt abundances and Pt/Os ratios of the parental melts for the Hawaiian volcanoes are similar (Fig. 11). These estimates suggest that hybridization of the mantle source with a pyroxenitic melt, and its associated BMS, either may not have played a major role in producing the trends observed between $^{187}Os/^{188}Os$ and $^{186}Os/^{188}Os$ ratios in the Hawaiian suite, or that the enriched Pt abundances in the source region somehow were not transferred to the parental melts for the picrites (Luguet et al., 2008).

6. Conclusions

1) The absolute HSE abundances of the Hawaiian picrites are intermediate between komatiites and typical MORB basalts. Osmium, Ir, and Ru behaved compatibly in the Hawaiian picrites, whereas Pt, Pd and Re generally behaved slightly incompatibly and became concentrated in the melt, although the behaviour of these elements was variable. The relative abundances of the HSE fall into two distinct groups that are not specific to a volcanic center. Type-1 patterns, when normalized to chondrites, are characterized by lower Pt/Ir, Pd/Ir and Pt/Pd than Type-2 samples.
2) The picrites analyzed in this study experienced variable amounts of olivine removal or accumulation, although some approximate a parental melt. This parental melt is estimated to contain ~16 wt.% MgO and ~11 wt.% Al_2O_3. The HSE characteristics of the various parental melts were generally similar (containing 0.5±0.2 ppb Os, 0.45±0.05 ppb Ir, 1.2±0.2 ppb Ru, 2.3±0.2 ppb Pt, and 0.35±0.05 ppb Re). The estimated parental melt for Hualalai has a higher Os content at 1.0 ppb. The Loihi parental melt contained lower abundances of Os, Ir and Ru, but higher Pt, Pd and Re contents.
3) Crustal processes probably had only a minor affect on the HSE abundances Hawaiian picrites. Volatile loss of Re (and perhaps Ir) may have occurred in some subaerially erupted lavas. If crustal contamination occurred, it had a minor effect on the absolute HSE abundances of the picritic suite.
4) The complex relationship between the degree of partial melting and crystal-liquid fractionation appears to be the dominant control on the observed HSE abundances in the samples. Type-1 and Type-2 HSE patterns reflect minor differences in residual sulfides left in the mantle source and/or the loss of IPGE during magma ascent or in the cumulate zones of higher-level magma chambers associated with chromite crystallization. Minor variations in the degree of partial melting can explain some of the differences in the absolute abundances of the HSE between volcanic centers (e.g. Loihi).
5) There are source heterogeneities among the Hawaiian volcanic centers which are reflected in the $^{187}Os/^{188}Os$ ratios observed. However, $^{187}Os/^{188}Os$ variations are a result of ancient processes and are decoupled from HSE abundances in parental melts. Any HSE heterogeneities in the mantle sources for the various Hawaiian volcanic centers are probably small and have been obscured by the partial melting and crystal-liquid fractionation processes. Melt percolation events may play a small role in the relative fractionation of Os, Ir and Ru and may be able to explain high Os/Ir and Os/Ru for Hualalai. These melt percolation events would have had to occur recently, so as not to disturb the long-term Re/Os and $^{187}Os/^{188}Os$ ratios of the system.

Acknowledgements

The authors would like to thank Don DePaolo for providing the HSDP samples, as well as Keith Putirka for sharing HSDP olivine data. Bill McDonough, Richard Ash and Igor Puchtel provided invaluable assistance with the various mass spectrometers, as well as Phil Piccoli with the electron microprobe. These individuals, as well as Ricardo Arevalo, also offered helpful discussions on the manuscript. Reviews from L. Reisberg and an anonymous journal reviewer greatly improved the quality of this manuscript, as did editor comments from B. Bourdon. This work was supported by NSF CSEDI grant 0330528 (to RJW), which is gratefully acknowledged.

References

Allègre, C.J., Moreira, M., 2004. Rare gas systematics and the origin of oceanic islands: the key role of entrainment at the 670 km boundary layer. Earth Planet. Sci. Lett. 228, 85–92.
Anderson, D.L., 1998. A model to explain the various paradoxes associated with mantle noble gas geochemistry. Proc. Natl. Acad. Sci. USA 95, 9087–9092.

Baker, J.A., Jensen, K.K., 2004. Coupled Os-186-Os-187 enrichments in the Earth's mantle—core–mantle interaction or recycling of ferromanganese crusts and nodules? Earth Planet. Sci. Lett. 220, 277–286.
Ballhaus, C., Bockrath, C., Wohlgemuth-Ueberwasser, C., Laurenz, V., Berndt, J., 2006. Fractionation of the noble metals by physical processes. Contrib. Mineral. Petrol. 152, 667–684.
Barnes, S.J., Picard, C.P., 1993. The behavior of platinum-group elements during partial melting, crystal fractionation, and sulfide segregation—an example from the Cape-Smith fold belt, northern Quebec. Geochim. Cosmochim. Acta. 57, 79–87.
Barnes, S.J., Naldrett, A.J., Gorton, M.P., 1985. The origin of the fractionation of platinum-group elements in terrestrial magmas. Chem. Geol. 53, 303–323.
Becker, H., Shirey, S.B., Carlson, R.W., 2001. Effects of melt percolation on the Re–Os systematics of peridotites from a Paleozoic convergent plate margin. Earth Planet. Sci. Lett. 188, 107–121.
Becker, H., Horan, M.F., Walker, R.J., Gao, S., Lorand, J.-P., Rudnick, R.L., 2006. Highly siderophile element composition of the Earth's primitive upper mantle: constraints from new data on peridotite massifs and xenoliths. Geochim. Cosmochim. Acta. 70, 4528–4550.
Bennett, V.C., Esat, T.M., Norman, M.D., 1996. Two mantle-plume components in Hawaiian picrites inferred from correlated Os-Pb isotopes. Nature 381, 221–224.
Bennett, V.C., Norman, M.D., Garcia, M.O., 2000. Rhenium and platinum group element abundances correlated with mantle source components in Hawaiian picrites: sulphides in the plume. Earth Planet. Sci. Lett. 183, 513–526.
Birck, J.-L., Roy-Barman, M., Capmas, F., 1997. Re–Os isotopic measurements at the femtomole level in natural samples. Geostand. Newsl. 21, 19–27.
Bizimis, M., Griselin, M., Lassiter, J.C., Salters, V.J.M., Sen, G., 2007. Ancient recycled mantle lithosphere in the Hawaiian plume: Osmium–Hafnium isotopic evidence from peridotite mantle xenoliths. Earth Planet. Sci. Lett. 257, 259–273.
Bockrath, C., Ballhaus, C., Holzheid, A., 2004. Fractionation of the platinum-group elements during mantle melting. Science 3053, 1951–1953.
Boyd, F.R., Mertzman, S.A., 1987. Composition of structure of the Kaapvaal lithosphere, southern Africa. In: Mysen, B.O. (Ed.), Magmatic Processes—Physicochemical Principles. The Geochemical Society, Special Publication #1, pp. 13–24.
Brandon, A.D., Walker, R.J., 2005. The debate over core–mantle interaction. Earth Planet. Sci. Lett. 232, 211–225.
Brandon, A.D., Norman, M.D., Walker, R.J., Morgan, J.W., 1999. ^{186}Os-^{187}Os systematics of Hawaiian picrites. Earth Planet. Sci. Lett. 174, 25–42.
Brandon, A.D., Walker, R.J., Puchtel, I.S., Becker, H., Humayun, M., Revillon, S., 2003. 186Os–187Os systematics of Gorgona Island komatiites: implications for early growth of the inner core. Earth Planet. Sci. Lett. 206, 411–426.
Brenan, J.M., McDonough, W.F., Dalpe, C., 2003. Experimental constraints on the partitioning of rhenium and some platinum-group elements between olivine and silicate melt. Earth Planet. Sci. Lett. 212, 135–150.
Brenan, J.M., McDonough, W.F., Ash, R., 2005. An experimental study of the solubility and partitioning of iridium, osmium and gold between olivine and silicate melt. Earth Planet. Sci. Lett., 237, 855–872.
Brügmann, G.E., Arndt, N.T., Hofmann, A.W., Tobschall, H.J., 1987. Noble-metal abundances in komatiite suites from Alexo, Ontario, and Gorgona Island, Colombia. Geochim. Cosmochim. Acta 51, 2159–2169.
Bryce, J.G., DePaolo, D.J., Lassiter, J.C., 2005. Geochemical structure of the Hawaiian plume: Sr, Nd, and Os isotopes in the 2.8 km HSDP-2 section of Mauna Kea volcano. Geochem. Geophys. Geosyst. 6, 1–36.
Büchl, A., Brügmann, G., Batanova, V.G., Münker, C., Hofmann, A.W., 2002. Melt percolation monitored by Os isotopes and HSE abundances: a case study from the mantle section of the Troodos Ophiolite. Earth Planet. Sci. Lett. 204, 385–402.
Büchl, A., Brügmann, G., Batanova, V.G., 2004a. Formation of podiform chromitite deposits: implications from PGE abundances and Os isotopic compositions of chromites from the Troodos complex, Cyprus. Chem. Geol. 208, 217–232.
Büchl, A., Brügmann, G., Batanova, V.G., Hofmann, A.W., 2004b. Os mobilization during melt percolation: the evolution of Os isotope heterogeneities in the mantle sequence of the Troodos Ophiolite, Cyprus. Geochim. Cosmochim. Acta 68, 3397–3408.
Campbell, I.H., Griffiths, R.W., 1990. Implications of mantle plume structure for the evolution of flood basalts. Earth Planet. Sci. Lett. 99, 79–93.
Chen, C.Y., Frey, F.A., Garcia, M.O., Dalrymple, G.B., Hart, S.R., 1991. The tholeiite to alkalic basalt transition at Haleakala volcano, Maui, Hawaii. Contrib. Mineral. Petrol. 106, 183–200.
Cohen, A.S., Waters, F.G., 1996. Separation of osmium from geological materials by solvent extraction for analysis by thermal ionization mass spectrometry. Anal. Chem. 332, 269–275.
Crocket, J.H., 2000. PGE in fresh basalt, hydrothermal alteration products, and volcanic incrustations of Kilauea volcano, Hawaii. Geochim. Cosmochim. Acta 64, 1791–1807.
Crocket, J.H., Macrae, W.E., 1986. Platinum-group element distribution in komatiitic and tholeiitic volcanic-rocks from Munro township, Ontario. Econ. Geol. 81, 1242–1251.
Danyushevsky, L.V., Della-Pasqua, F.N., Sokolov, S., 2000. Re-equilibration of melt inclusions trapped by magnesian olivine phenocrysts from subduction-related magmas: petrological implications. Contrib. Mineral. Petrol. 138, 68–83.
Eiler, J.M., Farley, K.A., Valley, J.W., Hofmann, A.W., Stolper, E.M., 1996. Oxygen isotope constraints on the sources of Hawaiian volcanism. Earth Planet. Sci. Lett. 144, 453–467.
Gaffney, A.M., Nelson, B.K., Reisberg, L., Eiler, J., 2005. Oxygen-osmium isotope systematics of West Maui lavas: a record of shallow-level magmatic processes. Earth Planet. Sci. Lett. 239, 122–139.
Garcia, M.O., Foss, D.J.P., West, H.B., Mahoney, J.J., 1995. Geochemical and isotopic evolution of Loihi Volcano, Hawaii. J. Petrol. 36, 1647–1674.
Gurriet, P.C. 1988, Geochemistry of Hawaiian dredged lavas. MSc Thesis, Massachusetts Institute of Technology.
Hauri, E.H., Kurz, M.D., 1997. Melt migration and mantle chromatography, 2: a time-series Os isotope study of Mauna Loa Volcano, Hawaii. Earth Planet. Sci. Lett. 153, 21–36.
Hauri, E.H., Lassiter, J.C., DePaolo, D.J., 1996. Osmium isotope systematics of drilled lavas from Mauna Loa, Hawaii. J. Geophys. Res. 101, 11793–11806.
Helz, R.T., 1987. Differentiation behavior of Kilauea Iki lava lake, Kilauea volcano, Hawaii: an overview of past and current work. In: Mysen, B.O. (Ed.), Magmatic Processes: Physicochemical Principles. The Geochemical Society Special Publication No. 1, pp. 241–258.
Horan, M.F., Walker, R.J., Morgan, J.W., Grossman, J.N., Rubin, A.E., 2003. Highly siderophile elements in chondrites. Chem. Geol. 196, 5–20.
Huang, S., Frey, F.A., 2003. Trace element abundances of Mauna Kea basalt from phase 2 of the Hawaii Scientific Drilling Project: petrogenetic implications of correlations with major element content and isotopic ratios. Geochem. Geophys. Geosyst. 4, 43.
Humayun, M., Qin, L.P., Norman, M.D., 2004. Geochemical evidence for excess iron in the mantle beneath Hawaii. Science 306, 91–94.
Jamais, M., Lassiter, J.C., Brügmann, G., 2008. PGE and Os isotopic variations in lavas from Kohala Volcano Hawaii: constraints on PGE behavior and melt/crust interaction. Chem. Geol. 250, 16–28.
Lassiter, J.C., 2003. Rhenium volatility in subaerial lavas: constraints from subaerial and submarine portions of the HSDP-2 Mauna Kea drillcore. Earth Planet. Sci. Lett. 214, 311–325.
Lassiter, J.C., Hauri, E.H., 1998. Osmium-isotope variations in Hawaiian lavas: evidence for recycled oceanic lithosphere in the Hawaiian plume. Earth Planet. Sci. Lett. 164, 483–496.
Luguet, A., Shirey, S.B., Lorand, J.P., Horan, M.F., Carlson, R.W., 2007. Residual platinum-group minerals from highly depleted harzburgites of the Lherz massif (France) and their role in HSE fractionation of the mantle. Geochim. Cosmochim. Acta 71, 3082–3097.
Luguet, A., Pearson, D.G., Nowell, G.M., Dreher, S.T., Coggon, J.A., Spetsius, Z.V., Parman, S.W., 2008. Enriched Pt–Re–Os isotope systematics in plume lavas explained by metasomatic sulfides. Science 319, 453–456.
Maier, W.D., Barnes, J., 2004. Pt/Pd and Pd/Ir ratios in mantle-derived magmas: a possible role for mantle metasomatism. S. Afr. J. Geol. 107, 333–340.
Maier, W.D., Roelofse, F., Barnes, S.J., 2003. The concentration of the platinum-group elements in south African komatiites: implications for mantle sources, melting regime and PGE Fractionation during crystallization. J. Petrol. 44, 1787–1804.
Marcantonio, F., Zindler, A., Elliott, T., Staudigel, H., 1995. Os isotope systematics of La Palma, Canary Islands—evidence for recycled crust in the mantle source of HIMU ocean islands. Earth Planet. Sci. Lett. 133, 397–410.
Martin, C.E., Carlson, R.W., Shirey, S.B., Frey, F.A., Chen, C.Y., 1994. Os isotopic variation in basalts from Haleakala volcano, Maui, Hawaii—a record of magmatic processes in oceanic mantle and crust. Earth Planet. Sci. Lett. 128, 287–301.
McDonough, W.F., 2003. Compositional model for the Earth's core, The Mantle and Core (ed. R.W. Carlson) Vol. 2 Treatise on Geochemistry (eds. H.D. Holland and K.K Turekian). Elsevier-Pergamon, Oxford, pp. 547–568.
Meisel, T., Walker, R.J., Irving, A.J., Lorand, J.-P., 2001. Osmium isotopic compositions of mantle xenoliths: a global perspective. Geochim. Cosmochim. Acta 65, 1311–1323.
Momme, P., Oskarsson, N., Keays, R.R., 2003. Platinum-group elements in the Icelandic rift system: melting processes and mantle sources beneath Iceland. Chem. Geol. 196, 209–234.
Montelli, R., Nolet, G., Dahlen, F.A., Masters, G., Engdahl, E.R., Hung, S.H., 2004. Finite-frequency tomography reveals a variety of plumes in the mantle. Science 303, 338–343.
Morgan, W.J., 1971. Convection plumes in the lower mantle. Nature 230, 42–43.
Nielsen, S.G., Rehkamper, M., Norman, M.D., Halliday, A.N., Harrison, D., 2006. Thallium isotopic evidence for ferromanganese sediments in the mantle source of Hawaiian basalts. Nature 439, 314–317.
Norman, M.D., Garcia, M.O., 1999. Primitive magmas and source characteristics of the Hawaiian plume: petrology and geochemistry of shield picrites. Earth and Planet. Sci. Lett. 168, 27–44.
Norman, M.D., Garcia, M.O., Bennett, V.C., 2004. Rhenium and chalcophile elements in basaltic glasses from Ko'olau and Moloka'i volcanoes: magmatic outgassing and composition of the Hawaiian plume. Geochim. Cosmochim. Acta 68, 3761–3777.
Pearson, D.G., Irvine, G.J., Ionov, D.A., Boyd, F.R., Dreibus, G.E., 2004. Re–Os isotope systematics and platinum group element fractionation during mantle melt extraction: a study of massif and xenolith peridotite suites. Chem. Geol. 208, 29–59.
Peuker-Ehrenbrink, B., Bach, W., Hart, S.R., Blusztajn, J.S., Abbruzzese, T., 2003. Rhenium–osmium isotope systematics and platinum group element concentrations in oceanic crust from DSDP/ODP Sites 504 and 417/418. Geochem. Geophys. Geosyst. 4, 1–28.
Pitcher, L., Helz, R.T., Walker, R.J., Piccoli, P, in press. Fractionation of the platinum-group elements and Re during crystallization of basalt in Kilauea Iki lava lake, Hawaii. Chem. Geol.
Puchtel, I., Humayun, M., 2000. Platinum group elements in Kostomuksha komatiites and basalts: implications for oceanic crust recycling and core–mantle interaction. Geochim. Cosmochim. Acta 64, 4227–4242.
Puchtel, I.S., Humayun, M., 2001. Platinum group element fractionation in a komatiitic basalt lava lake. Geochim. Cosmochim. Acta 65, 2979–2993.
Puchtel, I.S., Humayun, M., 2005. Highly siderophile element geochemistry of Os-187-enriched 2.8 Ga Kostomuksha komatiites, Baltic shield. Geochim. Cosmochim. Acta 69, 1607–1618.
Puchtel, I.S., Humayun, M., Campbell, A.J., Sproule, R.A., Lesher, C.M., 2004. Platinum group element geochemistry of komatiites from the Alexo and Pyke Hill areas, Ontario, Canada. Geochim. Cosmochim. Acta 68, 1361–1383.
Putirka, K.D., 2005. Mantle potential temperatures at Hawaii, Iceland, and the mid-ocean ridge system, as inferred from olivine phenocrysts: evidence for thermally driven plumes. Geochem. Geophys. Geosyst. 6, 1–14.

Putirka, K.D., Perfit, M., Ryerson, F.J., Jackson, M.G., 2007. Ambient and excess mantle temperatures, olivine thermometry, and active vs. passive upwelling. Chem. Geol. 241, 177–206.
Rehkamper, M., Halliday, A.N., Barfod, D., Fitton, J.G., 1997. Platinum-group element abundance patterns in different mantle environments. Science 278, 1595–1598.
Rehkamper, M., Halliday, A.N., Fitton, J.G., Lee, D.-C., Wieneke, M., Arndt, N.T., 1999. Ir, Ru, Pt and Pd in basalts and komatiites: new constraints for the geochemical behavior of the platinum group elements in the mantle. Geochim. Cosmochim. Acta. 63, 3915–3934.
Rhodes, J.M., 1996. Geochemical stratigraphy of lava flows sampled by the Hawaii Scientific Drilling Project. J. Geophys. Res. 101, 11729–11746.
Rhodes, J.M., Vollinger, M.J., 2004. Composition of basaltic lavas sampled by phase-2 of the Hawaii Scientific Drilling Project: geochemical stratigraphy and magma types. Geochem. Geophys. Geosyst. 5, 1–38.
Roeder, P.L., Emslie, R.F., 1970. Olivine-liquid equilibrium. Contrib. Mineral. Petrol. 29, 275–289.
Roy-Barman, M., Allégre, C.J., 1995. $^{187}Os/^{186}Os$ in oceanic island basalts—tracing oceanic crust recycling in the mantle. Earth Planet. Sci. Lett. 129, 145–161.
Schersten, A., Elliott, T., Hawkesworth, C., Norman, M., 2004. Tungsten isotope evidence that mantle plumes contain no contribution from the Earth's core. Nature 427, 234–237.
Shirey, S.B., Walker, R.J., 1995. Carius tube digestion for low-blank rhenium–osmium analysis. Anal. Chem. 67, 2136–2141.
Shirey, S.B., Walker, R.J., 1998. The Re–Os isotope system in cosmochemistry and high-temperature geochemistry. Ann. Rev. Earth Planet. Sci. 26, 423–500.
Sleep, N.H., 1990. Hotspots and mantle plumes—some phenomenology. J. Geophys. Res.-Solid Earth Planets 95, 6715–6736.
Sleep, N.H., 1992. Hotspot volcanism and mantle plumes. Annu. Rev. Earth Planet. Sci. 20, 19–43.
Smith, A.D., 2003. Critical evaluation of Re–Os and Pt–Os isotopic evidence on the origin of intraplate volcanism. J. Geodyn. 36, 469–484.
Snow, J.E., Schmidt, G., 1998. Constraints on Earth accretion deduced from noble metals in the oceanic mantle. Nature 391, 166–169.
Sobolev, A.V., Hofmann, A.W., Sobolev, S.V., Nikogosian, I.K., 2005. An olivine-free mantle source of Hawaiian shield basalts. Nature 434, 590–597.
Sobolev, A.V., Hofmann, A.W., Kuzmin, D.V., Yaxley, G.M., Arndt, N.T., Chung, S.L., Danyushevsky, L.V., Elliott, T., Frey, F.A., Garcia, M.O., Gurenko, A.A., Kamenetsky, V.S., Kerr, A.C., Krivolutskaya, N.A., Matvienkov, V.V., Nikogosian, I.K., Rocholl, A., Sigurdsson, I.A., Sushchevskaya, N.M., Teklay, M., 2007. The amount of recycled crust in sources of mantle derived melts. Science 316, 412–417.
Sun, W., Bennett, V.C., Eggins, S.M., Kamenetsky, V.S., Arculus, R.J., 2003. Enhanced mantle-to-crust rhenium transfer in undegassed arc magmas. Nature 422, 294–297.
Tanaka, R., Nakamura, E., Takahashi, E., 2002. Geochemical evolution of Koolau volcano, Hawaii. In: Takahashi, E., Lipman, P.W., Garcia, M.O., Naka, J., Aramaki, S. (Eds.), Hawaiian Volcanoes; Deep Underwater Perspectives. American Geophysical Union, Washington, DC, United States, pp. 311–332.
Tatsumi, Y., Oguri, K., Shimoda, G., 1999. The behaviour of platinum-group elements during magmatic differentiation in Hawaiian tholeiites. Geochem. J. 33, 237–247.
Walker, D., 2000. Core participation in mantle geochemistry: Geochemical Society Ingerson Lecture, GSA Denver, October 1999. Geochim. Cosmochim. Acta 64, 2897–2911.
Walker, R.J., Morgan, J.W., Horan, M.F., 1995. Os-187 enrichment in some plumes—evidence for core–mantle interaction. Science 269, 819–822.
West, H.B., Garcia, M.O., Gerlach, D.C., Romano, J., 1992. Geochemistry of tholeiites from Lanai, Hawaii. Contrib. Mineral. Petrol. 112, 520–542.
Widom, E., Shirey, S.B., 1996. Os isotope systematics in the Azores: implications for mantle plume sources. Earth Planet. Sci. Lett. 142, 279–296.
Wright, T.L., 1973. Magma mixing as illustrated by the 1959 eruption, Kilauea Volcano, Hawaii. Geol. Soc. Amer. Bull. 84, 849–858.
Yi, W., Halliday, A.N., Alt, J.C., Lee, D.C., Rehkamper, M., Garcia, M.O., Su, Y., 2000. Cadmium, indium, tin, tellurium and sulfur in oceanic basalts: implications for chalcophile element fractionation in the Earth. J. Geophys. Res. 105, 18927–18948.
Zoller, W.H., Parrington, J.R., Kotra, J.M.P., 1983. Iridium enrichment in airborne particles from Kilauea Volcano. Science 222, 1118–1121.